

# Immobilization of Chromium in Tannery Sludge Using Iron-Based Nanoparticles and Nanobiocomposites

M. Arthy · B. R. Phanikumar

Received: 15 December 2014 / Accepted: 22 May 2015 / Published online: 3 June 2015  
© Springer International Publishing Switzerland 2015

**Abstract** This paper presents the efficacy of zero-valent iron nanoparticles (ZVINs), magnetic iron oxide nanoparticles (MINs), zero-valent iron nanoparticles/sugarcane bagasse (ZVIN-SB) composite and magnetic iron oxide nanoparticles/sugarcane bagasse (MIN-SB) composite in immobilizing chromium present in tannery sludge. The optimized values for the immobilization of chromium by the adsorbents were found to be 48 h, 100 g/kg and 7, respectively, for time, adsorbent dosage and pH. The maximum uptake capacity was found to be 429.75, 539.25, 587.25 and 625.8 mg/kg, respectively, for ZVIN, MIN, ZVIN-SB and MIN-SB. The desorption study of the unamended sludge and sludge amended by ZVIN, MIN, ZVIN-SB and MIN-SB was carried out with three different desorbing media (0.1 N HCL, DIW and 0.1 N NaOH). It was found that the cumulative concentration of leachate chromium was more in basic condition than in neutral and acidic conditions. In column studies, the concentration of leachate

chromium attained 0 mg/L at 24, 15, 18 and 14 pore volumes, respectively, for the sludge amended by ZVIN, MIN, ZVIN-SB and MIN-SB. The experimental adsorption data fitted well with pseudo-first-order kinetics. The zero-order kinetics accurately predicted the experimental desorption capacity ( $q_e$ ) of the sludge amended by ZVIN, MIN, ZVIN-SB and MIN-SB. The Fourier transform infrared spectroscopy (FTIR) analysis showed that the amine, carboxyl, iron compounds, etc. present in the adsorbents were the chief causes for the immobilization of chromium. The X-ray diffraction (XRD) analysis of the sludge showed the presence of trivalent chromium compounds at a higher concentration.

**Keywords** Tannery sludge · Adsorbents · Immobilization of chromium · Desorption · Column studies · Kinetics

## Nomenclature

$q_t$	Amount of contaminant adsorbed/desorbed from sludge at time (min) (mg/kg)
$C_0$	Initial concentration of the chromium (mg/L)
$C_e$	Final concentration of the chromium (mg/L)
$V$	Volume of the solution (L)
$M$	Mass of the adsorbent (kg)
$C_t$ (mg/L)	Concentration of the contaminant in the liquid at varying contact time
$W$	Weight of the sludge (kg)
$R^2$	Correlation coefficient
$q_e$	Experimental uptake capacity/desorption capacity (mg/kg)

**Electronic supplementary material** The online version of this article (doi:10.1007/s11270-015-2466-7) contains supplementary material, which is available to authorized users.

M. Arthy (✉)  
Environmental, Water Resources and Transportation  
Engineering Division, School of Mechanical and Building  
Sciences, VIT University, Vellore 632 014, India  
e-mail: srjjart88@gmail.com

B. R. Phanikumar  
Department of Civil Engineering, School of Mechanical and  
Building Sciences, VIT University, Vellore 632 014, India  
e-mail: phanikumar\_29@yahoo.com

$q_{e,cal}$	Calculated uptake capacity/desorption capacity (mg/kg)
$k_1$	First-order kinetic rate constant (1/min)
$h$	Initial adsorption rate (mg/kg/min)
$t_{1/2}$	Half-life time (min)
$k_2$	Rate constant of pseudo-second-order equation (kg/mg/min)
$\alpha$	Elovich kinetic constant initial adsorption rate (mg/kg/min)
$\beta$	Elovich kinetic desorption constant (kg/mg)
$k$	Rate constant of the power function (mg/kg/min)
$k_v$	Power kinetic specific adsorption rate at unit time (mg/kg/min)
$k_0$	Zero-order rate constant (mg/kg/min)
$k_p$	Parabolic diffusion rate constant (kg/g/min <sup>0.5</sup> )

## 1 Introduction

Tanneries require a lot of water and chemicals for the process of making leather from raw skins/hides (Tunay et al. 1995). Chrome tannage with basic trivalent chromium salts has numerous technical advantages for converting putrescible collagen fibers into non-putrescible leather matrix than the mineral and organic tannage (Gong et al. 2010). Trivalent chromium in the leather exists as free, mono-coordinate or multi-coordinate state. The stability of the chromium increases as of the following order: free ions > mono-coordinate ions > multi-coordinate ions (Covington 1998). The oxidation of trivalent chromium is primarily associated with the chemical instability in the leather. Only 60 % of the chromium applied for tanning forms coordination bond with the peptide linkages of collagen fibres of skins/hides. The remaining unreacted chromium is discharged in the wastewater (Cassano et al. 1996). This leads to the discharge of large quantity of chromium-contaminated wastewater to the Common Effluent Treatment Plant (CETP). As a primary step, in CETP, the effluents from different tanneries were passed to equalization tank through screens, and it is chemically treated with lime and alum in the flash mixer. Polyelectrolyte is added in the baffle channel to facilitate coagulation and flocculation of solids which is sedimented in the primary clarifier. To precipitate the chromium as chromium hydroxide (Cr(OH)<sub>3</sub>), the higher pH values

were maintained in the primary clarifier. The precipitated chromium along with other organic compounds (primary chemical sludge) is then taken to the sludge drying beds (Chang et al. 2001). The wastewater after its primary treatment is processed biologically and passed through pressure sand filters and activated carbon filters to meet the discharge standards.

Though the effluent meets the discharge standards, the sludge from the primary and secondary clarifiers creates major environmental threats. Since, it is discharged as such to the landfill after dewatering without any further treatment. The major form of chromium present in the sludge is in the trivalent form. The disposal of chromium without any treatment leads to the oxidation under aerobic conditions. Oxidation of Cr<sup>3+</sup> to Cr<sup>6+</sup> was observed in the presence of oxidized manganese [MnOOH<sub>(s)</sub>] which served as electron acceptor in the reaction (Apte et al. 2006; Nakayama et al. 1981). It was found that the hexavalent form of chromium was 500 times more toxic than trivalent form (Costa 2003). Cr<sup>6+</sup> is not only toxic but also carcinogenic. As it is a strong oxidizing agent, it causes irritation to animal and plant tissues (Costa and Klein 2006). Though the Cr<sup>6+</sup> formed is ultimately reduced to Cr<sup>3+</sup> due to the presence of various reducing agents in the sludge, 17 % conversion of Cr<sup>3+</sup> to Cr<sup>6+</sup> is observed under aerobic conditions. This spreads the Cr<sup>6+</sup> pollution, due to rainfall, run-off and percolation (Apte et al. 2006). The slow conversion rate of Cr<sup>3+</sup> to Cr<sup>6+</sup> was observed in the natural environment in the wide pH range of 3–10 and PO<sub>2</sub> > 10<sup>-6</sup> atm (Apte et al. 2005).

The presence of chromium in polluted environment has been regulated and controlled by different environmental protection agencies around the world. The US Environmental Protection Agency (EPA) states that the maximum concentration value (MCV) of potable water should be 0.1 mg/L (Franco et al. 2009). Different treatment technologies such as phytoremediation, microbial remediation, chemical reduction, physical sorption (ion exchange resin, activated carbon, etc.), soil flushing and electrokinetic removal have been reported for the treatment of contaminated soil/sludges. The remediation of heavy metal-contaminated soil/sludges has been carried out with the main emphasis on immobilization technologies. Immobilization forms inert and highly insoluble metal species with soil/sludge amendments (Porter et al. 2004). Many immobilizing agents such as nanoscale zero-valent iron (nZVI) (Singh et al. 2012; Franco et al. 2009), polysaccharide-stabilized Fe–

Mn oxide nanoparticles (An and Zhao 2012), iron residues from water treatment (Nielsen et al. 2011), egg shell waste (Ahmad et al. 2012), pine bark (Park et al. 2008), etc. have been widely used by various researches to treat contaminated soils/sludges. Recently, nanoparticles and nanocomposites have been effectively utilized for the environmental applications. Wei et al. (2011) summarized various nanoparticle synthesizing methods with its unique physicochemical properties and its applications in various fields such as microwave absorption, environmental remediation, etc. In the aspect of environmental protection, the work carried out by various researchers on heavy metal removal especially on chromium using nanoparticles and nanocomposites has been discussed here briefly. Ferromagnetic carbon-coated Fe nanoparticles effectively removed 95 % of  $\text{Cr}^{6+}$  in wastewater via carbon shell physical adsorption (Zhang et al. 2010). Fe- $\text{Fe}_2\text{O}_3$ /polypropylene (pp) polymer nanocomposites (PNs) is introduced in synthesizing magnetic carbon nanocomposites (MCNs). The MCNs pyrolyzed from PNCs containing 20 % wt NP removes the  $\text{Cr}^{6+}$  completely from wastewater within 6 min. The adsorption capacity of the particles was found to be 1.5 mg/g (Zhu et al. 2012a, b, c). The removal of toxic hexavalent chromium has been investigated using magnetic polyaniline (PANI) polymer nanocomposites (Gu et al. 2012) and multi-walled carbon nanotubes (Gu et al. 2013). Gu et al. 2013 studied at pH 1, the  $\text{Cr}^{6+}$  solution completely oxidized MWNTs through the reduction of  $\text{Cr}^{6+}$  to  $\text{Cr}^{3+}$  over half an hour treatment. The hexavalent chromium removal by mesoporous magnetic carbon nanocomposite showed higher removal capacity of 3.74 mg/g with 10 min (Zhu et al. 2014). Carbon fabrics (CFs) loaded with PANI have demonstrated higher removal of  $\text{Cr}^{6+}$  within 15 min. The calculated maximum uptake capacity for 10 % PANI/CF was found to be 18.1 mg/g. Hexavalent chromium adsorbed on the surface of PANI/CF was then reduced to  $\text{Cr}^{3+}$  (Qiu et al. 2014a, b, c). Magnetic carbon nano-adsorbents (MC-O and MC-N) have demonstrated greater removal of hexavalent chromium. The adsorption capacities of MC-O and MC-N were found to be 293.8 and 327.5 mg/g, respectively (Qiu et al. 2014a, b, c). The hexavalent chromium removal was also investigated by magnetic carbon nanocomposites derived from cellulose at different carbonization temperatures. The specific surface area of the particles decreased with increasing temperature, heating rate and

retention time. The mechanism for the reduction of  $\text{Cr}^{6+}$  was found to be oxidation of carbon in neutral solutions as well as oxidation of ZVI in acidic solution (Qiu et al. 2015a, b). Magnetic graphene nanocomposites (MGNCs) showed extremely fast  $\text{Cr}^{6+}$  removal from wastewater with high removal efficiency. The complete removal of  $\text{Cr}^{6+}$  was observed using 3 g/L MGNCs within 5 min (Zhu et al. 2012a, b, c). The ethyl cellulose modified with 5, 10 and 20 wt% polyaniline (PANI/ECs) demonstrated a superior hexavalent chromium removal. The 20 % PANI loading removed 2 mg/L of  $\text{Cr}^{6+}$  completely within 5 min (Qiu et al. 2014a, b, c). Zhu et al. (2013) reviewed about the effective removal of heavy metals (Cr, As, Pd, Hg) using magnetic nanocomposites. Magnetic nanocomposites show great potential not only because they obtain high adsorption capacity but also the convenient recycling using permanent magnet (Zhu et al. 2013). The magnetic graphene nanoplatelet composites (MGNCs) decorated with core-shell Fe- $\text{Fe}_2\text{O}_3$  nanoparticles have shown high binding capacity of As(III). The adsorption capacity of MGNCs was found to be 11.34 mg/g (Zhu et al. 2012a, b, c). The activated carbon fabrics (ACFs) have removed the toxic hexavalent chromium ( $\text{Cr}^{6+}$ ). The  $\text{Cr}^{6+}$  in the aqueous solution was reduced to  $\text{Cr}^{3+}$  and adsorbed on the surface of ACFs at pH 1. The adsorption capacity of ACFs was found to be 5.59 mg/g (Xu et al. 2014). Qiu et al. (2015a, b) examined about the effective removal of  $\text{Cr}^{6+}$  by PANI-coated magnetic  $\text{Fe}_3\text{O}_4$ , carbon fabric and cellulose composites. The PANI improved the hydrophilicity of the adsorbents and enhanced the performance of  $\text{Cr}^{6+}$  reduction to  $\text{Cr}^{3+}$ .

This paper presents the efficacy of green-synthesized iron-based nanoparticles and nanobiocomposites in immobilizing chromium in tannery sludge. The treated sludge with and without adsorbents was subjected to desorption analysis in various types of environment such as acidic, basic and neutral conditions. The column study was carried out to analyse the leachability of chromium from the unamended sludge and sludge amended by nanoparticles and nanobiocomposites.

### 1.1 Objectives

The chief objectives of this study are the following:

- (i) To synthesize four different adsorbents, namely zero-valent iron nanoparticles (ZVINS), magnetic

iron oxide nanoparticles (MINs), zero-valent iron nanoparticles/sugarcane bagasse (ZVIN-SB) and magnetic iron oxide nanoparticles/sugarcane bagasse (MIN-SB) in a novel and green-mediated approach;

- (ii) To optimize various process parameters such as time, adsorbent dosage and pH for the immobilization of chromium in the sludge through batch study and to characterize the unamended sludge and sludge amended by ZVIN, MIN, ZVIN-SB and MIN-SB using X-ray diffraction (XRD), Fourier transform infrared spectroscopy (FTIR), scanning electron microscopy (SEM), energy dispersive X-ray spectroscopy (EDX) and cyclic voltammetry (CV);
- (iii) To establish the adsorption behaviour and kinetics of nanoparticles and nanobiocomposites ;
- (iv) To investigate the desorption behaviour of the unamended sludge and sludge amended by nanoparticles and nanobiocomposites through batch study and also to analyse the desorption kinetics and
- (v) To examine the leachate concentration of the unamended sludge and the sludge amended by nanoparticles and nanobiocomposites under dynamic condition.

## 2 Experimental Investigation

### 2.1 Materials and Methods

The chemicals used in the experimental programme were ferric chloride ( $\text{FeCl}_3$ ), sodium dodecyl sulphate ( $\text{NaC}_{12}\text{H}_{25}\text{SO}_4$ ), hydrochloric acid (HCL), sodium hydroxide (NaOH) and ammonia ( $\text{NH}_4\text{OH}$ ). They were obtained from sdfine-chem limited (SDFCL) and were all analytical reagent grades. All the working solutions were prepared with deionized water (DIW). The tea waste, sugarcane bagasse and neem leaves were collected from Vellore, TN, India. The primary sludge was collected from common effluent treatment plant near Ranipet, TN, India. It was dried and stored in air-tight container at 4 °C for further experimentation. The characterization of the sludge for various process parameters such as pH, electrical conductivity, chromium, chlorides, sulphates, calcium, sodium and total organic carbon is represented in Table 1.

**Table 1** Characteristics of primary sludge

Parameters	Values/quantity
Total chromium	24.2 g/kg
$\text{Cr}^{3+}$	23.23 g/kg
$\text{Cr}^{6+}$	0.968 g/kg
pH	8.54
Chlorides	8.52 g/L
Sulphates	54 mg/L
Calcium	102.44 mg/L
Sodium	13.35 g/L
Total organic carbon	205.8 g/L
Electrical conductivity	7.912 ms/cm
Chemical oxygen demand	1440 mg/L

### 2.2 Adsorbents

The iron-based nanoparticles such as ZVIN and MIN and nanobiocomposites such as ZVIN-SB and MIN-SB were used as adsorbents for the immobilization of total chromium in the sludge.

### 2.3 Preparation of the Adsorbents (Iron-Based Nanoparticles and Nanobiocomposites)

The adsorbents, namely ZVIN, ZVIN-SB, MIN and MIN-SB have been subjected to green synthesis using an effective and novel method. For the preparation of nanobiocomposites with ZVIN and MIN, the sugarcane bagasse was washed with ethanol and DIW. Then, it was oven-dried at 80 °C for 24 h. The oven-dried sugarcane bagasse was powdered and sieved. The particles smaller than 150  $\mu\text{m}$  size were used for preparing the nanobiocomposites. The nanoparticles and the nanobiocomposites were synthesized with the help of three solutions.

- Solution (1) The first solution was extracted from 26 g of tea waste in 1 L of DIW.
- Solution (2) The second solution was prepared by boiling 20 g of tea waste in 1 L of 0.2 M  $\text{FeCl}_3$  solution.
- Solution (3) The third solution was prepared by boiling 67 g of fresh neem leaves in 1 L of DIW water.

### 2.3.1 ZVIN Nanoparticles

One hundred seventy millilitre of 0.1 % sodium dodecyl sulphate (SDS) solution was mixed with 1 L of the solution (1) and stirred for 5 min. To the above mix, 0.1 N of FeCl<sub>3</sub> was added dropwise till the colour of the solution changed from orange to black. The solution was stirred at the temperature of 60 °C for 15 min. It was then oven-dried at 80 °C for 24 h. The dried particles were washed several times with DIW and ethanol. Finally, it was again oven-dried at the temperature of 80 °C.

### 2.3.2 ZVIN/SB Nanobiocomposite

The zero-valent nanobiocomposite was synthesized by using the same procedure as ZVIN nanoparticles with a minor variation. Before adding FeCl<sub>3</sub> and SDS solution, 3.3 g of sugarcane bagasse was added to 1 L of the solution (1). The solution was stirred in a magnetic stirrer for 10 min and later in a centrifuge for ten more minutes. The particles, which settled in the centrifuge, were collected and stirred with DIW and ethanol to remove the loosely bound particles. The particles were separated in a centrifuge and later oven-dried at 80 °C for 24 h.

### 2.3.3 MIN Nanoparticles

To 20 mL of the solution (2), 60 mL of 0.1 % SDS solution and 200 mL of ammonia (16.5 %) were added dropwise and stirred for 15 min at a temperature of 60 °C. The solution turned black immediately. The particles were separated using magnet. To increase the stability of the nanoparticles in the suspension, they were coated with the solution (3). The coated particles were washed several times with ethanol and DIW. The particles were then oven-dried for 15 h at 80 °C.

### 2.3.4 MIN/SB Nanobiocomposite

The magnetic iron nanobiocomposite was synthesized using the same procedure as MIN nanoparticles with the following modification. Sugarcane bagasse (0.4 g) was added to 20 mL of solution (2) and stirred for 10 min at 60 °C before adding 0.1 % SDS, ammonia (16.5 %) and neem leaf extract. The particles formed were separated using magnet and washed several times with ethanol

and DIW. The particles were then oven-dried at 80 °C for 15 h.

## 2.4 Batch Adsorption/Desorption Studies

The influence of individual variables such as pH, adsorbent dosage and time were investigated on the immobilization of the total chromium in the sludge. The optimization of the independent variables was done by varying the adsorbent dosage (50–150 g/kg), pH (6–11) and time (45 min–120 h). The shaking speed and temperature was maintained at 120 rpm and 30 °C, respectively. The adsorption experiments were carried out with 1 g of sludge in 15 mL of DIW. The uptake capacity of the adsorbents at different time periods can be calculated using the following Eq. (1):

$$q_t = (C_0 - C_e) * V / M \quad (1)$$

The desorption study was conducted by taking 1 g of sludge in 15 mL of desorbing medium (0.1 N HCL, 0.1 N NaOH and DIW). The amount of contaminant desorbed from the sludge for each reaction time was calculated by the following equation (Fonseca et al. 2009).

$$q_t = C_t V / W \quad (2)$$

The metal ion concentration in the desorbing medium was measured using Varian-AA240 atomic adsorption spectroscopy.

## 2.5 Column Studies

The leachate analysis of the treated sludge was studied under continuous flow of DIW. Totally, 8 g of amended and non-amended sludge were packed in the glass column of inner diameter 2 cm and height 7 cm. The schematic sketch of the column used in this study was given in the supplementary material (Fig. S1). Three layers of glass wool were placed in the column to avoid the disturbance of the influent flow and the sludge surface. The amended and non-amended sludge columns were saturated with DIW to reach field-holding capacity prior to leaching. The amount of water required for one pore volume was found to be 8.6, 8.6, 8.5, 8.4 and 8.4 mL, respectively, for control, ZVIN, MIN, ZVIN-SB and MIN-SB. The time required to collect one pore volume of leachate was found to be 27, 27, 25, 23 and 24 h, respectively, for ZVIN, MIN, ZVIN-SB

and MIN-SB. The DIW was applied to the top of each column at a rate of 0.5 mL/min at every 27, 27, 25, 23 and 24 h, respectively, for ZVIN, MIN, ZVIN-SB and MIN-SB. This leaching was continued up to 30 pore volumes. The leachates were collected and filtered through a 0.42  $\mu\text{m}$  Whatman filter paper for the analysis of chromium concentration in atomic adsorption spectroscopy.

## 2.6 Characterization of the Adsorbents and Sludge

The nanoparticles and nanobiocomposites were characterized using  $\text{pH}_{\text{pzc}}$ , UV, BET, XRD, FTIR, SEM, EDX, AFM and VSM (not shown in this paper). Figure S2 (a) and (b) show the particle size analysis of ZVIN and MIN nanoparticles. The particle size analysis was done by nanoparticle size analyser (SZ-100). The size of the particles was found to be 53.7 and 16.3 nm, respectively, for ZVIN and MIN. However, in AFM and SEM images, bigger particles were observed. This may be due to the agglomeration of ZVIN and MIN nanoparticles resulting in sizes of 296.8 and 263 nm, respectively. The AFM image showed triangular morphology for ZVIN and MIN particles. The sludge before and after the treatment process was characterized using SEM, EDX, XRD, FTIR and CV. The sludge collected after the treatment process was dried at 80 °C for 24 h, and it is stored in an air-tight container for further analysis. FEI Quanta FEG 200 scanning electron microscopy was used for scanning the surface and analysing the composition of the unamended sludge and sludge amended by nanoparticles and nanobiocomposites. The samples were sprinkled onto adhesive carbon tapes supported on metallic disks, and their images and elemental contents were recorded at different magnifications. For FTIR analysis, the samples were made as pellets with KBr, and they were then ground in an agate mortar. Shimadzu-IR-AFFINITY-1 spectrometer in the range of 500–4000  $\text{cm}^{-1}$  was used for identifying functional groups in the samples. The BRUKER's D8 advance instrument was used for XRD analysis. The source consisted of Cu K $\alpha$  radiation ( $\lambda=1.54187 \text{ \AA}$ ). Each sample was scanned in the  $2\theta$  range of 10°–80°. The cyclic voltammetry (CV) analysis of unamended sludge and sludge amended by nanoparticle and nanobiocomposites was done with the Cyclic Voltmeter Model CHI6003D. It is a three-electrode system consisting of platinum electrode as working electrode, Ag/AgCl as reference electrode and platinum wire as

counter electrode. The scan rate, high potential and low potential were assigned as 0.05 V/S, 1.6 and 0.6 V, respectively. The sludge before and after the treatment with nanoparticles and nanobiocomposites was digested for the analysis of valance state of chromium according to APHA 3030 D standard (APHA 1998).

## 3 Results and Discussion

### 3.1 Immobilization of Total Chromium in the Sludge: Batch Study

#### 3.1.1 Effect of Time

Figure 1a, b, c shows the effect of time on immobilization of total chromium in the sludge. The optimization of time was done by maintaining the adsorbent dosage and pH at 100 g/kg and 8.5, respectively, as constant. Figure 1a shows the effect of time on the percentage of Cr (total) retention by the adsorbents. The plot depicts that all the adsorbents attained the equilibrium at 48 h. The maximum chromium retaining efficiency at equilibrium time was found to be 42, 54, 59 and 63 %, respectively, for ZVIN, MIN, ZVIN-SB and MIN-SB. It was observed that the retention of chromium and the uptake capacity of the adsorbents were rapid up to a certain time period. This may be due to the availability of more vacant sites in the adsorbents (Mishra and Patel 2009). However, after this time period elapsed, there was no significant retention of chromium observed up to 120 h in the sludge by the adsorbents.

Figure 1b shows the effect of time on the uptake capacity of the adsorbents. The uptake capacity of ZVIN, MIN, ZVIN-SB and MIN-SB at 48 h was found to be 265.05, 340.65, 372.15 and 399.9 mg/kg, respectively. The uptake capacity increased with increase in time. It was observed that the leachability of the unamended sludge increased with increase in time (Fig. 1c). This increase in chromium concentration provides mass driving force to overcome the mass transfer resistance between the sludge slurry and the adsorbents. At 120 h, the maximum uptake capacity was found to be 429.75, 539.25, 587.25 and 625.8 mg/kg, respectively, for ZVIN, MIN, ZVIN-SB and MIN-SB. The uptake of chromium by the adsorbents was carried out in two phases. The first phase involved the early speedy uptake because of the surface adsorption. The second phase involved slow uptake because of the transport of

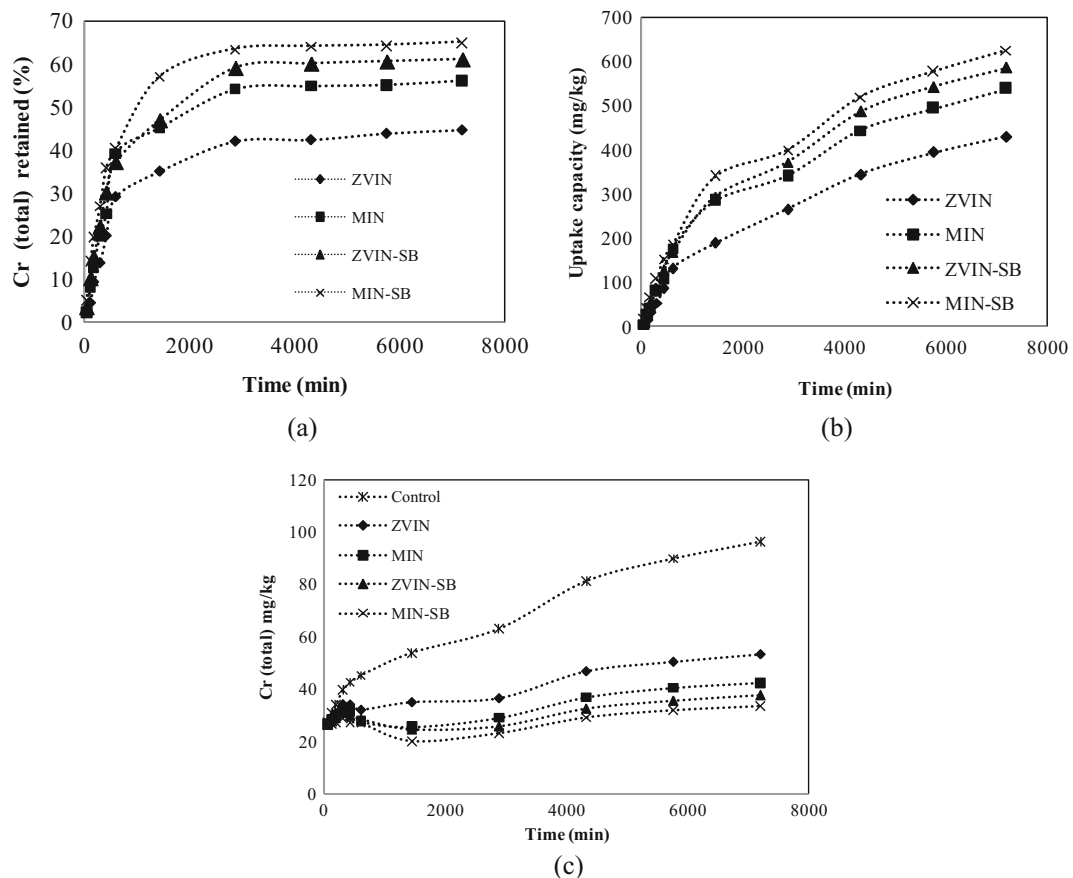


**Fig. 1** Effect of time on **a** percentage of Cr (total) retention, **b** uptake capacity and **c** leaching of Cr (total) from primary sludge with iron-based nanoparticles and nanobiocomposites

chromium ions on the adsorbents through external film diffusion or intraparticle diffusion which includes diffusion on pore wall surface and pore diffusion of chromium into the adsorbents (Weber and Smith 1987). Other researchers (Foo and Hameed 2011; Cossich et al. 2002; Sing and Yu 1998; Volesky and Holan 1995; Ceribasi and Yetis 2001) also found similar results.

Figure 1c shows the effect of time on the leaching of chromium from the unamended sludge and the sludge amended by ZVIN, MIN, ZVIN-SB and MIN-SB. As the time increased, the leachability of the chromium increased for both the types of sludge. The leachate concentration for the unamended sludge increased from 27.36 mg/kg (45 min) to 96.27 mg/kg (7200 min) whereas for the sludge amended by ZVIN, MIN, ZVIN-SB and MIN-SB the maximum leachate concentration at 7200 min (120 h) was respectively found to be 53.29, 42.34, 37.54 and 33.69 mg/kg.

### 3.1.2 Effect of Adsorbent Dosage

Figure 2a, b, c shows the effect of adsorbent dosage on the immobilization of total chromium in the sludge. The optimization was carried out at normal sludge pH (8.5) and equilibrium time (48 h). Figure 2a shows the effect of adsorbent dosage on the percentage of chromium retention by the adsorbents. The result depicts that, as the adsorbent dosage increases up to 100 g/kg, retention of chromium by the adsorbents increased. The increase in dosage beyond 100 g/kg did not show any significant change in retaining the chromium present in the sludge. At 100 g/kg, the maximum retaining efficiency was found to be 42, 54, 59 and 63.4 %, respectively, for ZVIN, MIN, ZVIN-SB and MIN-SB. Figure 2b shows the uptake capacity of the adsorbents in the removal of chromium from the sludge at different dosages. Uptake capacity decreased with increase in adsorbent dosage.

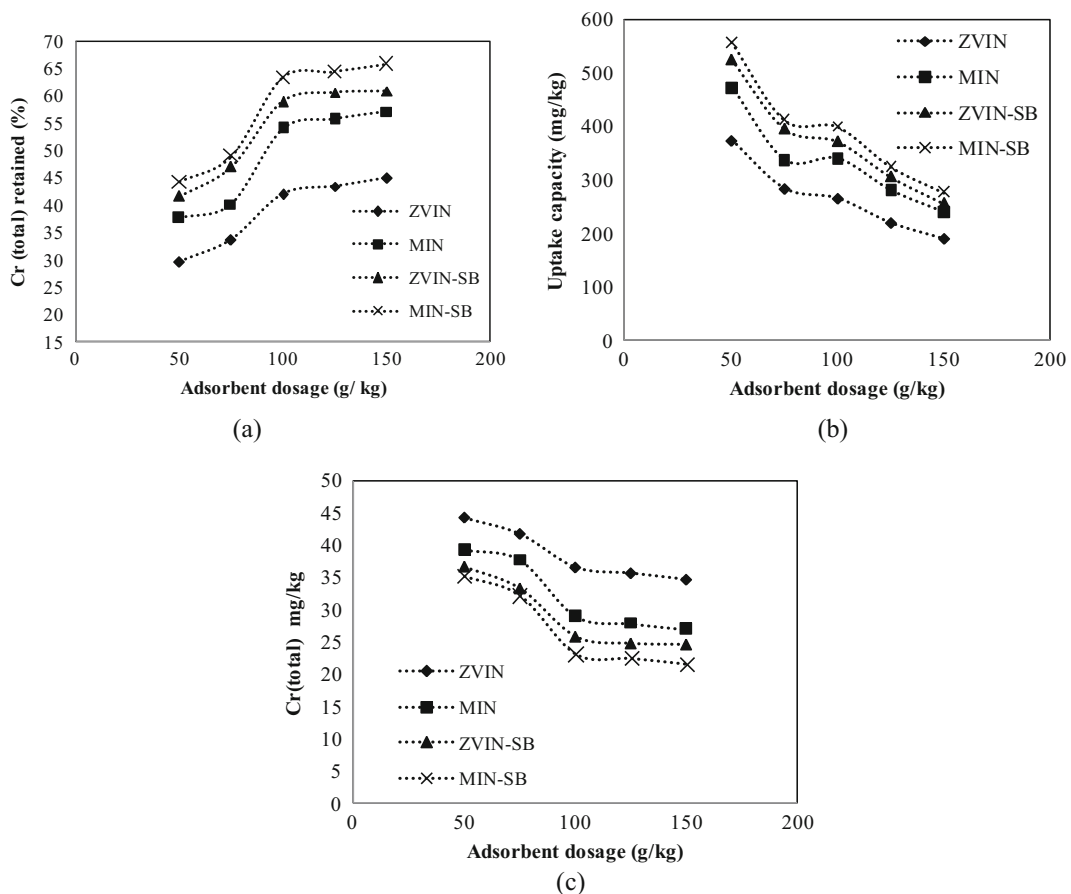
This may be because of (i) utilization of lower adsorptive capacity of the adsorbents during adsorption process and (ii) decrease in the surface area of the adsorbents due to the overlapping of active sites at higher dosage (Manohar et al. 2002).

Figure 2c shows the leachability of chromium from the unamended sludge and the sludge amended by ZVIN, MIN, ZVIN-SB and MIN-SB at varying adsorbent dosage. Chromium concentration in the leachate from the unamended sludge was found to be 63.075 mg/kg. The plot shows that, for the amended sludge (50 g/kg), the concentration of chromium in the leachate was found to be 44.37, 39.36, 36.79 and 35.19 mg/kg, respectively, for ZVIN, MIN, ZVIN-SB and MIN-SB. As dosage increased up to 100 g/kg, the leachability of chromium from the sludge decreased, and further increase in dosage did not show any significant reduction in the chromium leachate concentration.

At the optimum adsorbent dosage, the leachate concentration was found to be 36.57, 29.01, 25.86 and 23.08 mg/kg, respectively, for ZVIN, MIN, ZVIN-SB and MIN-SB.

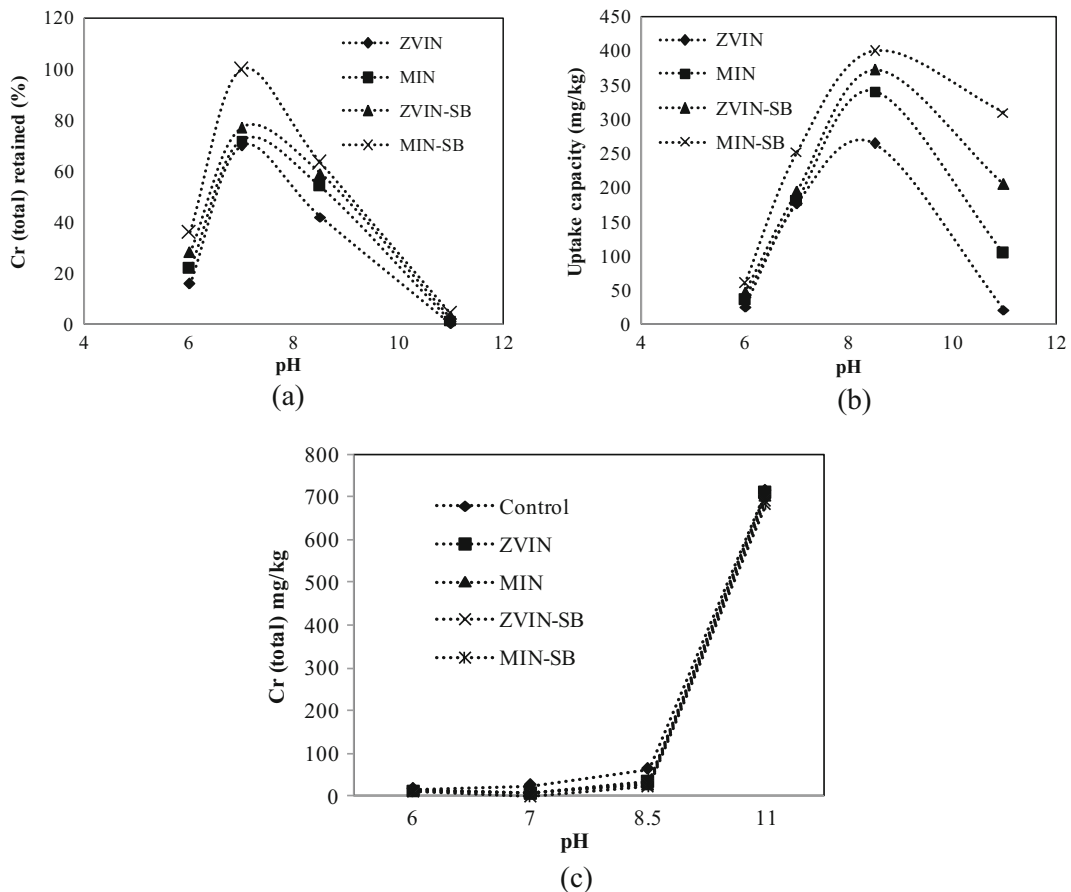
### 3.1.3 Effect of pH

Figure 3a, b, c shows the effect of pH on the immobilization of total chromium in the sludge by ZVIN, MIN, ZVIN-SB and MIN-SB. The pH of solution is one of the important parameters since it influences the surface charge and dissociation of the functional groups on the adsorbents. pH also alters the degree of ionization and speciation of the metal ions (Reddy and Lee 2013). The normal pH of the sludge was found to be 8.5. When removal of trivalent chromium was attempted with ZVIN, MIN, ZVIN-SB and MIN-SB in aqueous phase, the maximum removal efficiency was obtained at pH 6.



**Fig. 2** Effect of adsorbent dosage on **a** percentage of Cr (total) retention, **b** uptake capacity and **c** leaching of Cr (total) from primary sludge by iron-based nanoparticles and nanobiocomposites





**Fig. 3** Effect of pH on **a** percentage of Cr (total) retention, **b** uptake capacity and **c** leaching of Cr (total) from primary sludge by iron-based nanoparticles and nanobiocomposites

Hence, the effect of pH on the chromium retention by adsorbents was studied in the pH range between 6 and 11. Figure 3a shows that at pH 7, the adsorbents retained the maximum quantity of chromium present in the sludge. The percentage of retention at the optimum pH was found to be 69.9, 72, 77 and 100 %, respectively, for ZVIN, MIN, ZVIN-SB and MIN-SB. Figure 3b shows that, as pH increased from 6 to 8.5, the uptake capacity of the adsorbents increased, but further increase of pH from 8.5 to 11 decreased the uptake capacity of the adsorbents. At pH 8.5, the uptake capacity was found to be 265.05, 340.65, 372.15 and 399.9 mg/kg, respectively, for ZVIN, MIN, ZVIN-SB and MIN-SB.

Figure 3c shows that, as pH increased from 6 to 7, the leachability of chromium from the amended sludge decreased and further increase in pH increased the leachability of chromium from the sludge. The leachate concentration from the amended sludge at the optimum

pH was found to be 7.59, 7.08, 5.81 and 0 mg/kg, respectively, for ZVIN, MIN, ZVIN-SB and MIN-SB. The leaching concentration of the unamended sludge was found to be 16.39, 25.29, 63.09 and 715.47 mg/kg, respectively, for pH of 6, 7, 8.5 and 11.

### 3.1.4 Possible Mechanism in the Adsorption of Chromium Ions by the Adsorbents

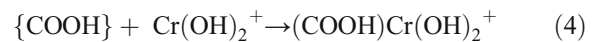
The major chromium species present in the sludge was found to be  $\text{Cr}^{3+}$  (96 %) and  $\text{Cr}^{6+}$  (4 %). The trivalent species would be in different forms such as  $\text{Cr}^{3+}$ ,  $\text{Cr}(\text{OH})^{2+}$ ,  $\text{Cr}(\text{OH})_2^+$ ,  $\text{Cr}(\text{OH})_3$  and  $\text{Cr}(\text{OH})_4^-$  at various pH values. At pH 6, chromium would be in the form of  $\text{Cr}(\text{OH})^{2+}$  and  $\text{Cr}(\text{OH})_2^+$ . At pH 7, the predominant chromium species would be  $\text{Cr}(\text{OH})_2^+$  and the neutral species ( $\text{Cr}(\text{OH})_3^0$ ) begin to appear. The  $\text{Cr}(\text{OH})^{2+}$  and  $\text{Cr}(\text{OH})_2^+$  are octahedral ligands with one or two

hydroxide ligands. At pH values above 9, the major trivalent chromium species would be in neutral species  $\text{Cr}(\text{OH})_3^0$  and the anionic species ( $\text{Cr}(\text{OH})_4^-$ ) begin to appear (Kumar et al. 2009; Rivera-Utrilla and Sanchez-Polo 2003). The point of zero charge of ZVIN, MIN, ZVIN-SB and MIN-SB was found to be 4, 7.1, 4.5 and 6.8, respectively. When  $\text{pH} < \text{pH}_{\text{pzc}}$ ,  $\text{pH} = \text{pH}_{\text{pzc}}$ ,  $\text{pH} > \text{pH}_{\text{pzc}}$ , the surface charge of the adsorbent would be positive, neutral and negative. Thus, at optimum pH 7, the surface charge of the adsorbents would be negative. This condition favours the adsorption of positively charged chromium species on the adsorbents. Specifically, at pH higher than 3–4 and 5.5, the carboxylic and amine groups would be deprotonated. Thus, the  $\text{Cr}(\text{OH})_2^+$  are bound to nanoparticles and nanobiocomposites through amine and carboxylic groups.

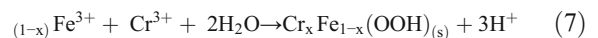
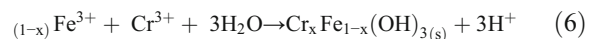
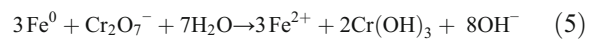
The increase in retention and the uptake capacity up to pH 8.5 is due to the presence of positively charged chromium species  $\text{Cr}(\text{OH})_2^+$  and neutral species  $\text{Cr}(\text{OH})_3^0$  in an equal concentration. The negatively charged adsorbents attract the positively charged chromium species. Further increase in pH dominated the neutral and anionic chromium species, and hence, the uptake capacity decreases after pH 8.5. At higher pH value (i.e. at 11), the chromium ions become anionic. Thus, at a pH of 11, the repulsion between the negatively charged chromium species and the negatively charged adsorbents decreases the percentage of chromium retention and the uptake capacity of the adsorbents. Moreover, at a pH above 10, hydroxides act as bridging ligands, forming multi-nuclear species  $[(\text{H}_2\text{O})_4\text{Cr}(\text{OH})_2\text{Cr}(\text{H}_2\text{O})_4]^{4+}$ . This bridging structure decreases the adsorption of chromium at higher pH (Kumar et al. 2009).

Among all the adsorbents, the MIN-SB showed the highest retention capacity. The MIN-SB also showed higher adsorption response, when the adsorbents were tried for the removal of trivalent chromium ions from the aqueous solution. This may be due to the involvement of major functional groups present in MIN-SB in the retention of chromium ions. The FTIR study of the raw adsorbents showed the presence of functional groups such as  $\text{NH}_2$ ,  $\text{OH}$ ,  $\text{COOH}$ ,  $\text{C}=\text{O}$ ,  $\text{C}-\text{O}$ ,  $\text{C}-\text{H}$ ,  $\text{C}-\text{S}$ ,  $\text{SO}_3$ ,  $\text{FeOOH}$ ,  $\text{FeO}$ ,  $\text{Fe}_2\text{O}_3$  and  $\text{Fe}_3\text{O}_4$  (figures not shown). Though the functional groups of all the adsorbents involved in the adsorption of chromium from aqueous solution, the major

stretch and shift of the functional groups appeared in MIN-SB. The presence of these functional groups in adsorbents encouraged the adsorption of chromium ions through ion exchange and hydrogen bonding, apart from electrostatic attraction. Equations (3) and (4) given below represent ion exchange and hydrogen bonding respectively.



The following reactions also take place in the retention of chromium by the adsorbents.



where  $x$  varies from 0 to 1. The solubility of  $\text{Cr}_x\text{Fe}_{1-x}(\text{OH})$  is much lower than that of  $\text{Cr}(\text{OH})_3$ .  $\text{Cr}^{3+}$  may also precipitate in the form of  $\text{Cr}_x\text{Fe}_{1-x}(\text{OOH})$  (Cao and Zhang 2006). The 4 % hexavalent chromium present in the tannery sludge would have reacted with iron particles to produce  $\text{Cr}(\text{OH})_3$  according to Eq. (5). Similar study was done by Singh et al. 2011 for the removal of hexavalent chromium from chromium-spiked soil using zero-valent iron nanoparticles. Equations (6) and (7) represent the possible reactions between the trivalent chromium species and the adsorbents.

### 3.2 Leachate Analysis: Batch Study

#### 3.2.1 Desorption Study of the Unamended Sludge and Sludge Amended by Nanoparticles and Nanobiocomposites

The desorption experiments were carried out in order to mimic the field conditions wherein the treated sludge gets exposed to various environmental conditions. Desorption represents the emission of chemical species from the solid surface. The reasons for desorption may be (i) the emission of the species by breaking its bond with surface atoms without chemical conversion and (ii) the emission of new molecules from a chemical reaction

of the species (association or decomposition). The desorption rate depends on the density of the chemical species, the strength of the bonding and the surface temperature. The desorption of chromium from the unamended sludge and sludge amended by nanoparticles and nanobiocomposites was carried out with 0.1 N HCL, DIW and 0.1 N NaOH. The control represents that the desorption study was carried out with the unamended sludge (maintained at the optimized conditions (pH 7, time 48 h)).

*Desorption Study of the Sludge in Acidic (0.1 N HCL) Condition* Figure 4a, b represents the analysis of chromium desorption from the unamended sludge and sludge amended by nanoparticles and nanobiocomposites in acidic condition with respect to time. Figure 4a shows the percentage of chromium retention by the adsorbents in acidic condition. At 5 h (300 min), the percentage of chromium (total) retained by the adsorbents was found to be 18.77, 30.99, 31.14 and 32.2 %, respectively, for ZVIN, MIN, ZVIN-SB and MIN-SB. The plot shows that as time increases, the percentage of chromium retention by the adsorbents increases and reached 100 % at 72 h (4320 min). Further increase in time also showed 100 % retention of chromium by the adsorbents in the sludge. Figure 4b shows the leachability of the unamended sludge and sludge amended by nanoparticles and nanobiocomposites. As time increases, the leachability from the unamended sludge increases from 9.825 mg/kg (5 h) to 21.465 mg/kg (96 h) whereas the adsorbents in the sludge decreased the leachability of the chromium and reached zero leaching at 72 h (4320 min). The cumulative leachate concentration of chromium was found to be 89.79, 21.84, 19.80, 18.95 and 16.38 mg/kg, respectively, for control, ZVIN, MIN, ZVIN-SB and MIN-SB. The percentage of chromium retention in the cumulative leachate concentration was found to be 75.6, 77.94, 78.8 and 81.7 %, respectively, for ZVIN, MIN, ZVIN-SB and MIN-SB.

*Desorption Study of the Sludge in Neutral (DIW) Condition* Figure 4c, d represents the analysis of chromium desorption from the unamended sludge and sludge amended by nanoparticles and nanobiocomposites in neutral condition. Figure 4c shows the percentage of chromium retention by the adsorbents in neutral condition. At 5 h (300 min), the percentage of chromium retention was found to be 31, 25.17, 9.99 and 84.85 %, respectively, for ZVIN, MIN, ZVIN-SB and MIN-SB.

The 100 % retention of chromium by the adsorbents was observed at 96, 48, 72 and 48 h, respectively, for ZVIN, MIN, ZVIN-SB and MIN-SB. The leachability of the unamended and amended sludge in neutral condition was represented in Fig. 4d. The leachability of unamended sludge increases from 42.78 mg/kg (5 h) to 91.68 mg/kg (120 h). At 5 h, the leachability of chromium from the amended sludge was found to be 29.505, 32.01, 38.505 and 6.48 mg/kg, respectively, for ZVIN, MIN, ZVIN-SB and MIN-SB. The cumulative leachate concentration was 433.11, 60.75, 55.75, 86.445 and 9.675 mg/kg, respectively, for control, ZVIN, MIN, ZVIN-SB and MIN-SB. The percentage of retention by adsorbents in cumulative chromium concentration was 85.97, 87.12, 80.04 and 97.76 %, respectively, for ZVIN, MIN, ZVIN-SB and MIN-SB.

*Desorption Study of the Sludge in Basic (0.1 N NaOH) Condition* Figure 4e, f represents the analysis of chromium desorption from the unamended sludge and sludge amended by nanoparticles and nanobiocomposites in basic condition. The percentage of chromium retention by the adsorbents was represented in Fig. 4e at basic condition. The results show that, in basic condition, the 100 % retention of chromium by the adsorbents was not achieved even after 216 h. The equilibrium time in the desorption of chromium ions from the sludge amended by nanoparticles and nanobiocomposites was achieved at the end of 168 h. At 168 h, the percentage of retention was found to be 97.84, 98, 98.21 and 98.78 %, respectively, for ZVIN, MIN, ZVIN-SB and MIN-SB. Further increase in time after 168 h has shown only little difference in the retention of chromium by the adsorbents. Figure 4f shows the leachability of the unamended sludge and sludge amended by nanoparticles and nanobiocomposites in basic condition.

The leachability of the unamended sludge was found to increase from 118.41 mg/kg (5 h) to 214.8 mg/kg (216 h) whereas for the amended sludge, the leachability was found to decrease with increase in time. At 168 h, the leachability of chromium from the amended sludge was found to be 3.45, 3.15, 2.85 and 1.95 mg/kg, respectively, for ZVIN, MIN, ZVIN-SB and MIN-SB. Further increase in time shows that the release of chromium from the amended sludge gets saturated, and it does not lead to 0 mg/kg concentration of chromium in the leachate. The cumulative leachate concentration was found to be 1593.495, 502.08,

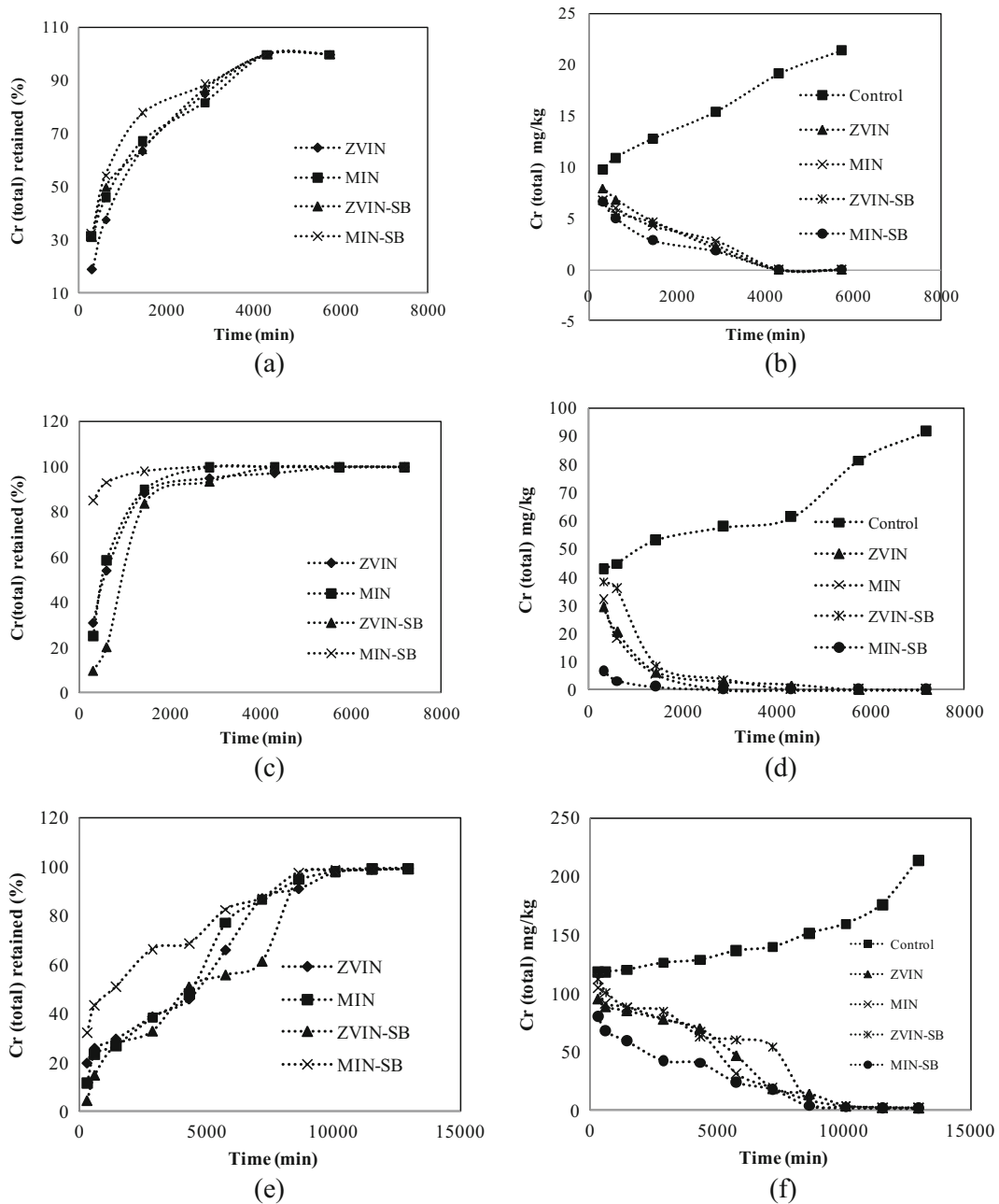


**Fig. 4** Desorption analysis of the treated primary sludge: (i) percentage of Cr (total) retained by the adsorbents in various conditions (a acidic, c neutral and e basic) and (ii) leachability of chromium in various conditions (b acidic, d neutral and f basic)

494.58, 577.695 and 338.67 mg/kg, respectively, for control, ZVIN, MIN, ZVIN-SB and MIN-SB. It was observed that the adsorbents have reduced the leachate concentration up to 68.4, 68.9, 63.7 and 78.7 %, respectively, by ZVIN, MIN, ZVIN-SB and MIN-SB.

*Effect of Desorption on the Adsorbents* Figure 5 represents the desorption effects of the adsorbents at various conditions. Figure 5a shows the retention capacity of the adsorbents with respect to time during desorption process in acidic condition. The plot shows that the retention capacity of the adsorbents increases with increase in

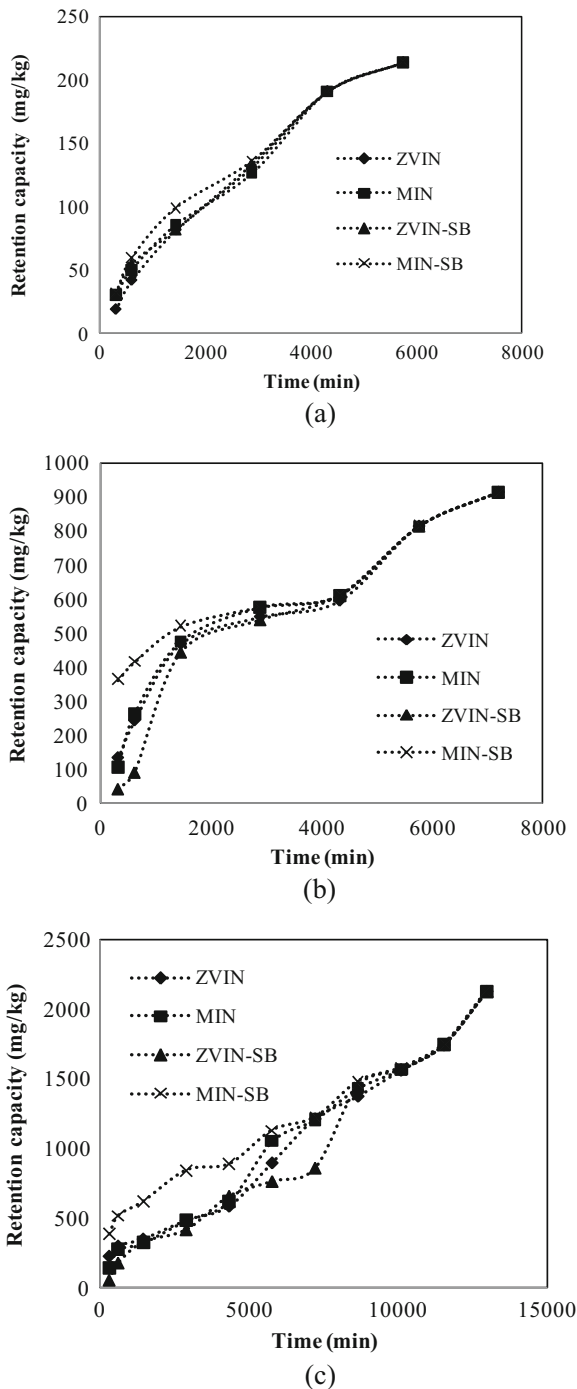


**Fig. 5** Retention capacity of the adsorbents during desorption process in various conditions (**a** acidic, **b** neutral and **c** basic)

time. At fifth hour, the retention capacity of the adsorbents was found to be 18.45, 30.45, 30.6 and 31.65 mg/kg, respectively, for ZVIN, MIN, ZVIN-SB and MIN-SB. At 96th hour, the retention capacity of all

the adsorbents was found to be 214.65 mg/kg. Figure 5b shows the retention capacity of the adsorbents at various time periods in neutral condition. At fifth hour, the retention capacity of the adsorbents was observed as 132.75, 107.7, 42.75 and 363 mg/kg, respectively, for ZVIN, MIN, ZVIN-SB and MIN-SB. The maximum retention capacity of the adsorbents in neutral condition was 916.8 mg/kg at 120th hour. Figure 5c shows the retention capacity of the adsorbents in basic condition. At 5th hour, the retention capacity of ZVIN, MIN, ZVIN-SB and MIN-SB was 232.8, 136.05, 52.65 and 383.1 mg/kg, respectively. At 216th hour, the maximum retention capacity of the adsorbents was found to be 2131.35, 2131.05, 2132.7 and 2134.95 mg/kg, respectively, for ZVIN, MIN, ZVIN-SB and MIN-SB.

*Possible Mechanism in the Desorption of Chromium from Tannery Sludge* The maximum desorption of chromium in all desorbing media was rapid initially, and later, the velocity of the desorption started decreasing. When adsorption energy is considerably high, the desorption process is limited by the transport rate of contaminants that move from the surface layer to sub-layer. Hence, it can be concluded that the chromium present in the low energy sites are easily and quickly desorbed when compared with the strongly adsorbed chromium (Labib et al. 2010) (Wang and Grathwohl 2009). The desorption study of the unamended and amended sludge clearly shows that the addition of ZVIN, MIN, ZVIN-SB and MIN-SB have reduced the chromium concentration in the leachate. This might be due to the involvement of major functional groups present in the adsorbents in the retention of chromium ions present in the tannery sludge. The FTIR study (Fig. S3) also portrayed that major stretch and shift of the peaks in the amended sludge. In particular, the decrease in intensities and shift of COOH and COO<sup>-</sup> groups were observed in amended sludge. This is due to the availability of binding sites for Cr<sup>3+</sup> in carboxyl and carbonyl groups. This suggests that the retention of Cr ions occurs through complexation reaction involving carboxylate groups (Fonglim et al. 2008). Specifically out of all adsorbents, the MIN-SB has shown higher chromium retention in all desorbing media. The percentage of retention by the adsorbents with respect to cumulative leachate concentration under various desorption media followed the order DIW > 0.1 N HCL > 0.1 N NaOH. This may be due to the following facts:

- (i) The addition of water to the treated sludge did not alter the pH of the slurry. Hence, the chromium species present in the slurry will be in the form of  $\text{Cr}(\text{OH})_2^+$  at this condition. Since this form of chromium ions has much affinity towards the negatively charged adsorbents, the desorption of chromium ions from the adsorbents was found to be less when DIW was added as desorbing media.
- (ii) The addition of acid to the treated sludge has reduced the pH of the slurry to 5.9. The chromium species at this pH will be positively charged ( $\text{Cr}(\text{OH})^{2+}$  and  $\text{Cr}(\text{OH})_2^+$ ). At this pH, the surface of ZVIN and ZVIN-SB will be negatively charged whereas the surface of MIN and MIN-SB was found to be less protonated. Hence, apart from electrostatic attraction, the hydrogen bonding of chromium ions with the adsorbents also reduced the desorption of chromium ions from the sludge, when 0.1 N HCL was added as desorbing media.
- (iii) The addition of 0.1 N NaOH has increased the pH of the slurry to 8.2. At this pH, the chromium species will be in the form of  $\text{Cr}(\text{OH})_3^0$  and  $\text{Cr}(\text{OH})_2^+$ . Hence, due to the presence of less cationic charged chromium species, the desorption of the chromium from the amended sludge was found to be comparatively high at this condition.

The lesser desorption of chromium ions from adsorbents may be due to the following reasons: (i) According to the classification of metal ions,  $\text{Cr}^{3+}$  was considered to be hard acid. This hard acid forms strong and stable complex with strong base amine ( $-\text{NH}_2$ ) present in the adsorbents, and (ii) the formation of bidentate and tridentate coordinate bond between  $\text{Cr}^{3+}$  and adsorbents which is more difficult to break (Kumar et al. 2009).

### 3.3 Leachate Analysis of the Unamended Sludge and Sludge Amended with Nanoparticles and Nanobiocomposites: Column Study

The chromium mobility from the unamended sludge and sludge amended by ZVIN, MIN, ZVIN-SB and MIN-SB was studied in the downward movement. Figure 6a shows that the highest chromium concentration occurred in the first leaching event for all the samples. The highest amount of leaching was observed in all leaching experiments for the unamended sludge. At the first pore volume, the chromium concentration

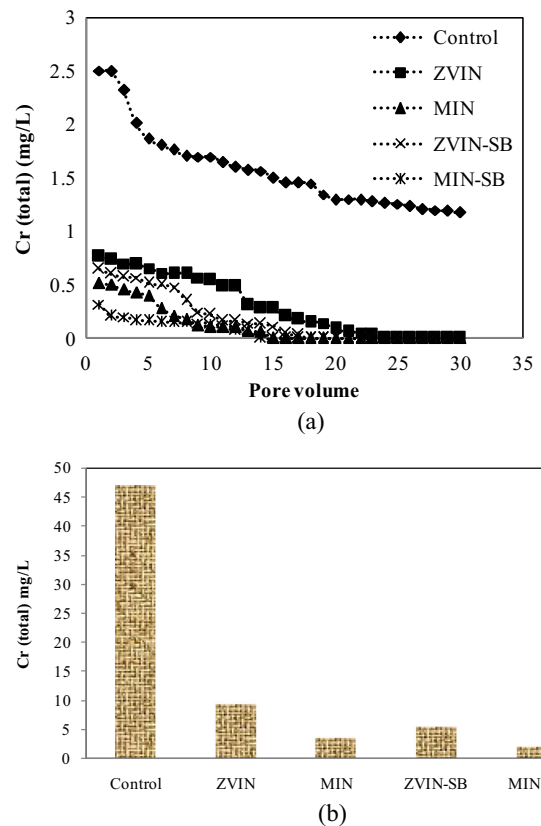


**Fig. 6** Column study of the unamended sludge/control and sludge amended by nanoparticles and nanobiocomposites. **a** Leaching concentration of chromium and **b** cumulative chromium concentration

was found to be 2.506, 0.768, 0.513, 0.643 and 0.317 mg/L, respectively, for the unamended sludge and sludge amended by ZVIN, MIN, ZVIN-SB and MIN-SB. At the 30th pore volume, the leachate concentration of chromium from the unamended sludge was found to be 1.174 mg/L. The sludge amended by nanoparticles and nanobiocomposites attained 0 mg/L leaching at 24, 15, 18 and 14 pore volumes, respectively, for ZVIN, MIN, ZVIN-SB and MIN-SB. Thus, the results show that, with increase in pore volume, the sludge amended by ZVIN, MIN, ZVIN-SB and MIN-SB significantly reduced the concentration of chromium in the leachate. This was evident with batch desorption study when 0.1 N HCL and DIW were used as desorbing media. The leaching was observed in two different phases for the unamended sludge and sludge amended by nanoparticles and nanobiocomposites. The first phase showed a rapid decrease, and the second

phase indicated a slow decrease in the concentration of chromium in leachate.

Figure 6b shows the cumulative leachate chromium concentration of the unamended sludge and sludge amended by ZVIN, MIN, ZVIN-SB and MIN-SB under dynamic condition. The results show that the cumulative leachate concentration was found to be 47.22, 9.21, 3.52, 5.46 and 2.01 mg/L, respectively, for unamended sludge and sludge amended by ZVIN, MIN, ZVIN-SB and MIN-SB. The percentage of chromium retention by the adsorbents with respect to cumulative leachate concentration was found to be 80.49, 92.5, 88.4 and 95.74 %, respectively, for ZVIN, MIN, ZVIN-SB and MIN-SB.

### 3.3.1 Column Leaching Kinetics

The kinetic parameters and rate controlling step for the leaching of chromium from tannery sludge through distilled water can be analyzed according to the heterogeneous reaction models (Levenspiel 1972). The kinetics was described by a two-stage model of chemical reaction followed by diffusion stage (Kim et al. 2014). The fractional conversion  $X$  is given by the following equation:

$$X = \frac{\text{Amount of chromium in the solution}}{\text{Total amount of chromium in the original sample}} \quad (8)$$

and at any time  $t$ , the integrated equations for fluid–solid heterogeneous reactions are

$$1-(1-X)^{1/3} = k_{c,chem}t \quad (9)$$

$$1-3(1-X)^{2/3} + 2(1-X) = k_{c,product}t \quad (10)$$

where  $k_{c,chem}$  and  $k_{c,product}$  are constants for chemical reaction and diffusion stage. Figure S3 (a) and (b) show the fractional conversion of chromium during leaching and the relationship between  $1-(1-X)^{1/3}$  and reaction time during chemical reaction stage. Figure S3 (c) shows the relationship between  $1-3(1-X)^{2/3}+2(1-X)$  and reaction time during the diffusion stage. The plot shows that, as time increases, the leachability of chromium decreases for unamended sludge and sludge amended by nanoparticles and nanobiocomposites. The leaching of chromium up to a certain time period followed the initial rapid chemical reactions and then diffusion stage.

## 3.4 Evaluation of the Experimental Data

### 3.4.1 Adsorption Kinetic Models

The experimental adsorption data was evaluated with four kinetic models such as pseudo-first-order (Nandi et al. 2009), pseudo-second-order (Ho and Mckay 1999), Elovich (Errais et al. 2011) and power (Basha and Murthy 2007). The linearized equations of the kinetic models were given by the following equations:

$$\text{Pseudo-first-order equation : } \ln(q_e - q_t) = \ln(q_{e,cal}) - k_1t \quad (11)$$

$$\text{Pseudo-second-order equation : } t/q_t = (1/k_2q_{e,cal}^2) + (t/q_{e,cal}) \quad (12)$$

$$\text{Elovich : } q_t = (1/\beta)\ln(\alpha\beta) + (1/\beta)\ln t \quad (13)$$

$$\text{Power : } \ln q_t = \ln k + v \ln t \quad (14)$$

The first-order kinetic parameters, calculated adsorption capacity ( $q_{e,cal}$ ) and first-order constant ( $k_1$ ), can be obtained by the plot  $\ln(q_e - q_t)$  vs  $t$ . The parameter  $h$  and  $t_{1/2}$  show the evaluation of initial adsorption rate and time at which half of the adsorption process is completed. Parameters  $h$  and  $t_{1/2}$  are given by the following equations:

$$h = k_1q_{e,cal}^2 \quad (15)$$

$$t_{1/2} = 0.693/k \quad (16)$$

The pseudo-second-order kinetic parameters calculated adsorption capacity ( $q_{e,cal}$ ) and second-order constant ( $k_2$ ) can be obtained from the plot  $t/q_t$  vs  $t$ . Elovich model assumes heterogeneous active sites of the adsorbent and the production of activation energy during the adsorption (Gerente et al. 2007). The two constants, namely initial adsorption rate ( $\alpha$ ) and the extent of surface coverage ( $\beta$ ), can be obtained from the plot  $q_t$  vs  $\ln t$ . The power functional model is a modified form of Freundlich equation. The constants fractional power kinetic model ( $K$ ) and specific adsorption rate at unit time ( $kv$ ) can be estimated from the plot of  $\ln q_t$  vs  $\ln t$ .

### 3.4.2 Desorption Kinetic Models

The experimental desorption data were evaluated using zero-order, first-order, second-order, parabolic diffusion, power and simple Elovich model (Dang et al. 1994; Rashti et al. 2014; Fonseca et al. 2009). The linearized kinetic model can be given by the following equation:

$$\text{Zero-order equation : } q_t = q_{e,\text{cal}} - k_0 t \quad (17)$$

$$\text{First-order equation : } \ln q_t = \ln q_{e,\text{cal}} - k_1 t \quad (18)$$

$$\text{Second-order equation : } 1/q_t = 1/q_{e,\text{cal}} - k_2 t \quad (19)$$

$$\text{Parabolic diffusion : } q_t = q_{e,\text{cal}} - k_p t^{0.5} \quad (20)$$

$$\text{Power : } \ln q_t = \ln k + \nu \ln t \quad (21)$$

$$\text{Simple Elovich : } q_t = 1/\beta \ln \alpha \beta + 1/\beta \ln t \quad (22)$$

The zero-, first- and second-order constants, calculated desorption capacity ( $q_{e,\text{cal}}$ ) and kinetic constants ( $k_0$ ,  $k_1$ ,  $k_2$ ) can be obtained from the plot  $q_t$  vs  $t$ ,  $\ln t$  vs  $t$  and  $1/q_t$  vs  $t$ , respectively. The parabolic diffusion, power and Elovich constants can be obtained from the plot  $q_t$  vs  $t^{0.5}$ ,  $\ln q_t$  vs  $\ln t$  and  $q_t$  vs  $\ln t$ , respectively.

### 3.4.3 Adsorption Kinetics of the Nanoparticles and Nanobiocomposites

The assessment of the kinetic model was done by  $R^2$ . Table 2 shows the value of kinetic parameters for the adsorption of total chromium on ZVIN, MIN, ZVIN-SB and MIN-SB. The suitability of kinetic model was assessed based on  $R^2$  value greater than 0.95. Comparatively, among all the adsorption kinetic models, the pseudo-first-order kinetics described the adsorption data effectively. This was consistent with the previous research on  $\text{Cr}^{6+}$  reduction and immobilization (Singh et al. 2011). The calculated  $q_{e,\text{cal}}$  value by pseudo-first-order equation was found to be 427.686, 521.078, 577.004 and 596.232 mg/kg, respectively, for ZVIN, MIN, ZVIN-SB and MIN-SB. The calculated  $q_{e,\text{cal}}$

value from pseudo-first-order kinetic model suits the experimental  $q_e$  value. The kinetic adsorption rate describes the adsorption capacity of adsorbent in unit time (Lu et al. 2014). The average value of  $k_1$  was  $4 \times 10^{-4}$ ,  $4.1 \times 10^{-4}$ ,  $4.2 \times 10^{-4}$  and  $4.2 \times 10^{-4}$  (1/min), respectively, for ZVIN, MIN, ZVIN-SB and MIN-SB. The higher  $k_1$  value for MIN-SB indicated the enhanced retention rate of chromium ions.

The parameter  $h$  is widely used for the evaluation of initial adsorption rate.  $t_{1/2}$  represents the time at which half of the adsorption process is completed. The  $h$  value obeyed the following order: MIN-SB (149.3 (mg/kg/min)) > ZVIN-SB (139.83 (mg/kg/min)) > MIN (111.32 (mg/kg/min)) > ZVIN (73.166 (mg/kg/min)). This indicates that the MIN-SB immobilized chromium ions better than ZVIN-SB, ZVIN and MIN. The smallest  $t_{1/2}$  indicates fastest adsorption (Tseng et al. 2011). The ZVIN-SB and MIN-SB showed a lesser  $t_{1/2}$  value which indicated that the nanobiocomposites involved in a quick retention of chromium present in the sludge. It is evident from  $R^2$  value (0.76) that the adsorption data of ZVIN does not describe the pseudo-second-order kinetic model in an effective manner. The values of Elovich constants,  $\alpha$  and  $\beta$ , are shown in Table 2. The increase in " $\alpha$ " and decrease in " $\beta$ " indicates quicker retention of chromium ions by the adsorbents. The Elovich constant values indicate that MIN-SB has a high  $\alpha$  value and a low  $\beta$  value, which indicates that among all adsorbents, MIN-SB has the greatest affinity towards chromium ions. The  $\nu$  value was found to be less than 1 which indicates that the power function model has satisfactorily described the time-dependent chromium adsorption on the adsorbents. The similar result was obtained when  $\text{Cr}^{6+}$  was adsorbed on chemically modified seaweed (Basha and Murthy 2007). The values of  $k\nu$  represents the specific adsorption rate at unit time which followed the order as MIN-SB > ZVIN-SB > MIN > ZVIN.

### 3.4.4 Desorption Kinetics of the Sludge

Desorption kinetics is determined to evaluate the reversibility of the contaminant to the extraction media. The zero-order, first-order, second-order, Elovich, parabolic diffusion and power kinetic model were analyzed to study the desorption kinetics. The experimental desorption capacity ( $q_e$ ) of the treated primary sludge with various desorbing media was given in the supplementary file (Fig. S4). Figure S4(a) shows the experimental



**Table 2** Adsorption kinetics of iron-based nanoparticles and nanobiocomposites

Kinetic model	Parameters	ZVIN	MIN	ZVIN-SB	MIN-SB
Pseudo-first order	$q_{e,cal}$	427.686	521.078	577.004	596.232
	$k_1$	0.00040	0.00041	0.00042	0.00042
	$h$	73.166	111.32	139.83	149.30
	$t_{1/2}$	1732.5	1690.24	1650	1650
	$R^2$	0.984	0.986	0.987	0.985
Pseudo-second order	$q_{e,cal}$	680.272	386.100	793.651	763.359
	$k_2$	$3.55 \times 10^{-7}$	$1.21 \times 10^{-5}$	$4.58 \times 10^{-7}$	$6.49 \times 10^{-7}$
	$R^2$	0.760	0.969	0.937	0.975
Elovich	$\alpha$	0.829	1.126	1.226	1.417
	$\beta$	0.012	0.009	0.009	0.008
	$R^2$	0.923	0.938	0.931	0.940
Power	$k$	0.297	0.427	0.728	1.308
	$V$	0.868	0.859	0.799	0.735
	$kV$	0.258	0.367	0.581	0.961
	$R^2$	0.944	0.930	0.953	0.952

desorption capacity ( $q_e$ ) of the unamended sludge and sludge amended by nanoparticles and nanobiocomposites in acidic condition. It was found that, for unamended sludge, the leachability of chromium increases with increase in time (9.82 mg/kg (5 h)–21.465 mg/kg (96 h)), whereas for sludge amended by nanoparticles and nanobiocomposites, the experimental desorption capacity decreases and becomes zero at 72 h. Figure S4(b) shows the experimental desorption capacity ( $q_e$ ) of the unamended sludge and sludge amended by nanoparticles and nanobiocomposites in neutral condition. At 5 h (300 min), the experimental desorption capacity was found to be 42.78, 26.82, 29.1, 35.0 and 5.89 mg/kg, respectively, for unamended sludge and sludge amended by ZVIN, MIN, ZVIN-SB and MIN-SB. Figure S4(c) shows the experimental desorption capacity in basic condition. It shows that desorption of sludge amended by nanoparticles and nanobiocomposites gets saturated at 168 h. At 168 h, the experimental desorption capacity ( $q_e$ ) was found to be 159.945, 3.13, 2.86, 2.591 and 1.77 mg/kg, respectively, for unamended sludge and sludge amended by ZVIN, MIN, ZVIN-SB and MIN-SB. The results show more desorption of chromium in unamended sludge than sludge amended by nanoparticles and nanobiocomposites. Desorption of chromium was the least in sludge amended by MIN-SB in various conditions.

Table 3 represents desorption rate constants of the kinetic models. The kinetic models were assessed based on the  $R^2$  ( $>0.95$ ) value. Based on  $R^2$  value, the zero-order kinetic model was found to be less effective for desorption data of sludge amended by nanoparticles and nanobiocomposites when water was used as desorbing media. ZVIN-SB amended sludge in basic condition and MIN-SB amended sludge in acidic condition also portrayed a less suitability of zero-order kinetics. The calculated desorption capacity ( $q_{e,cal}$ ) of all types of amended sludge from zero-order kinetics showed less deviation from experimental desorption ( $q_e$ ) values. Based on  $q_{e,cal}$  values, the zero-order kinetics was found to be better than other kinetic models. Table 3 shows the  $q_{e,cal}$  values of the sludge amended by nanoparticles and nanobiocomposites under different types of environment.

The first-order kinetic model suited well for ZVIN, MIN and ZVIN-SB amended sludge when acid was used as desorbing media. In neutral condition, the first-order model was found to be effective for MIN and MIN-SB amended sludge. The first-order model did not describe the desorption data effectively when 0.1 N NaOH was used as desorbing medium. The values of the second-order kinetic parameters  $q_{e,cal}$  and  $k_2$  indicate that it is not suitable for the evaluation of experimental data. The applicability of zero-order and first-order kinetics than second-order kinetics indicates

that for all adsorbents, the chromium ions present in the outer surface was desorbed. A similar result was obtained when copper ions were desorbed from magnetic polymer adsorbent (Tseng et al. 2009). According to Elovich kinetic model, the increase in  $\alpha$  and decrease in  $\beta$  value indicate an increase in desorption rate of chromium ions from the sludge amended by nanoparticles and nanobiocomposites. Thus, the sludge amended by MIN and ZVIN-SB has higher  $\alpha$  and lower  $\beta$  values when 0.1 N NaOH was used as desorbing medium. This shows that the MIN and ZVIN-SB have higher desorption capacity in basic condition. This was evident from the experimental ( $q_e$ ) value of MIN (95.27 mg/kg) and ZVIN-SB (102.85 mg/kg). Desorption of chromium ions from all the adsorbents was more in basic condition than in neutral and acidic conditions.

### 3.5 Characterization of Unamended Sludge and Sludge Amended by Nanoparticles and Nanobiocomposites

#### 3.5.1 FTIR Spectroscopy

The Fourier spectral analysis of unamended sludge and sludge amended by ZVIN, MIN, ZVIN-SB and MIN-SB was given in the supplementary file (Fig. S5). Table 4 shows the functional groups present in the sludge before and after treatment with adsorbents. The following observations can be made for unamended sludge and the sludge amended by nanoparticles and nanobiocomposites.

- (i) The peaks observed in the range 3300–3500  $\text{cm}^{-1}$  indicate the N–H stretching from secondary amine and characteristic stretching vibration of O–H bond (Lu et al. 2010; Farinella et al. 2007). The alteration of pH in the raw sludge (Fig. S5(b)) indicated the shift in peak from 3442.94 to 3452.58  $\text{cm}^{-1}$  and the appearance of new peak at 3417.86  $\text{cm}^{-1}$ . The change in intensity and shift of the peaks to lower wavelength within this region in the sludge amended by nanoparticles and nanobiocomposites (Fig. S5(c) to (f)) is due to the metal binding. The similar observation was obtained when  $\text{Hg}^{2+}$  was adsorbed onto palm shell powder (Kushwaha et al. 2012).
- (ii) The peaks in the range between 2500 and 3300  $\text{cm}^{-1}$  indicated the O–H bond stretching from carboxylic acids (Mohan 2004). The change in intensity and the shift of peaks were observed in

amended sludge. This indicates the involvement of overlapped O–H and C–H bonds from carboxylic acid in the retention of chromium ions.

- (iii) The peaks in the range 1580–1650 and 1535–1640  $\text{cm}^{-1}$  represent the N–H in plane bending vibration from primary amine and C=O stretching, respectively (Mohan et al. 2006).
- (iv) The peaks between 1430 and 1455  $\text{cm}^{-1}$  is due to  $\text{CH}_3$  bending vibration (Mohan 2004). The peaks in this range were observed only in the raw sludge. For the unamended sludge and sludge amended by nanoparticles and nanobiocomposites, the peaks were not observed in this region. Thus, the change in pH of the raw sludge would have altered this functional group. The addition of acid to the raw sludge would have reacted with the methyl groups presented in the sludge. Hence, the disappearance of the peaks was observed for the unamended sludge and sludge amended by nanoparticles and nanobiocomposites.
- (iv) The peaks between 1300 and 1430  $\text{cm}^{-1}$  (Fig. S5) are due to  $\text{COO}^-$  symmetric stretching of carboxylates (Mohan 2004).
- (v) The peaks between 1020 and 1220  $\text{cm}^{-1}$  indicate the C–N stretching of alkyl amine (Mohan 2004). The shift of the peak to the lower wave number and change in intensities of peaks in sludge amended by nanoparticles and nanobiocomposites indicate the deterioration of the alkyl amine group on the adsorption of chromium ions on the adsorbents.
- (vi) The stretch and shift of the peaks between 810 and 950  $\text{cm}^{-1}$  indicate the asymmetric stretching of C–H groups (Mohan 2004).
- (vii) The peaks between 700 and 750  $\text{cm}^{-1}$  indicate the out-of-plane bending vibration of N–H groups, which is due to N–H wagging and twisting from aliphatic secondary amine. The peaks between 600 and 800  $\text{cm}^{-1}$  indicate stretching vibration of C–S bond (Mohan 2004).
- (viii) The peaks in the range 565–625, 450–550 and 520–610  $\text{cm}^{-1}$  were respectively found to be O–N=O bending, S–S stretching and iron oxide (Lu et al. 2010; Mohan 2004).

The alteration of pH in the raw sludge resulted in the modification of functional groups. This was evident from the spectral analysis of the raw sludge (Fig. S5(a)) and the unamended sludge (Fig. S5(b)). For the sludge amended by ZVIN, ZVIN-SB and

**Table 3** Description kinetics of the sludge amended by iron-based nanoparticles and nanobiocomposites

Kinetic model	Parameters	ZVIN-amended sludge			MIN-amended sludge			ZVIN-SB-amended sludge			MIN-SB-amended sludge		
		Acid <sup>a</sup>	Water <sup>b</sup>	Base <sup>c</sup>	Acid <sup>a</sup>	Water <sup>b</sup>	Base <sup>c</sup>	Acid <sup>a</sup>	Water <sup>b</sup>	Base <sup>c</sup>	Acid <sup>a</sup>	Water <sup>b</sup>	Base <sup>c</sup>
Zero order	$K_0$	0.001	0.005	0.008	0.001	0.019	0.009	0.001	0.012	0.009	0.001	0.003	0.006
	$q_{e,cal}$	7.498	21.860	91.110	6.284	32.28	94.58	6.318	36.470	101.700	6.579	6.273	65.700
	$R^2$	0.976	0.727	0.964	0.956	0.924	0.967	0.974	0.828	0.936	0.766	0.852	0.960
First order	$q_{e,cal}$	8.358	24.850	133.312	6.636	44.617	142.955	7.028	45.784	161.641	7.045	8.375	101.801
	$K_1$	0.00048	0.00071	0.00030	0.00034	0.00155	0.00033	0.00044	0.00096	0.00032	0.00054	0.00154	0.00035
Second order	$R^2$	0.999	0.927	0.855	0.991	0.997	0.909	0.973	0.941	0.753	0.911	0.979	0.889
	$q_{e,cal}$	12.421	-30.684	-30.211	7.542	-46.816	-24.426	10.087	-49.801	20.060	9.796	-11.148	-13.353
	$K_2$	-0.00013	-0.00015	-0.00002	-0.00009	-0.00016	0.00002	-0.00014	-0.00011	0.00003	-0.00018	-0.00078	-0.00004
Elovich	$R^2$	0.975	0.992	0.541	0.999	0.985	0.615	0.937	0.988	0.559	0.991	0.995	0.635
	$\alpha$	18.336	72.330	209.005	14.039	101.783	232.275	14.684	112.897	232.591	18.835	20.390	171.488
	$\beta$	0.049	0.012	0.004	0.064	0.009	0.004	0.061	0.008	0.004	0.047	0.0429	0.005
Parabolic diffusion	$R^2$	0.979	0.946	0.755	0.988	0.993	0.825	0.934	0.916	0.770	0.952	0.962	0.931
	$K_p$	0.14185	0.51334	1.02281	0.10051	1.13788	1.15081	0.11121	0.96722	1.10396	0.1481	0.2269	0.83516
	$q_{e,cal}$	9.6925	31.492	113.211	7.85376	47.14898	120.3387	8.01524	51.91033	125.8817	9.00374	9.274	85.26804
Power	$R^2$	0.999	0.849	0.899	0.994	0.965	0.938	0.972	0.895	0.887	0.868	0.9121	0.983
	$K$	$1.6 \times 10^2$	$1.8 \times 10^4$	$2.5 \times 10^4$	60.920	$2.2 \times 10^4$	$4.8 \times 10^4$	$1.06 \times 10^2$	$2.6 \times 10^4$	$4.4 \times 10^4$	$3.18 \times 10^2$	$1.74 \times 10^4$	$4.2 \times 10^4$
	$V$	-0.531	-1.114	-0.853	-0.389	-1.153	-0.943	-0.482	-1.111	-0.914	-0.661	-1.38634	-0.976
$R^2$	0.913	0.985	0.570	0.957	0.978	0.629	0.848	0.933	0.518	0.999	0.893	0.649	

**Table 4** FTIR analysis of unamended sludge and sludge amended by iron-based nanoparticles and nanobiocomposites

Functional groups	Raw sludge	Unamended sludge	ZVIN-amended sludge	MIN-amended sludge	ZVIN-SB-amended sludge	MIN-SB-amended sludge
N–H stretching (2°—amine) and O–H bond	3442.94	3452.58 3417.86	3415.93	3415.93	3415.93	3415.93
Carboxylic acid O–H bonded stretching	2960.73 2926.01 2854.65	3234.64 2927.94 2854.65	3236.55 2926.01 2854.65	3142.04 2926.01 2854.65	3257.77 3236.55 2926.01 2854.65	3236.55 2927.94 2854.65
N–H in plane bending (1° amine free) and C=O stretching	1641.42 1629.85	1641.42 1627.92	1641.42 1627.92	1641.42 1625.99	1627.92	1618.28
CH <sub>3</sub> bending	1440.83 1431.18	–	–	–	–	–
COO <sup>−</sup> symmetric stretching	1381.03	1402.25	1402.25	1409.96	1402.25	1402.25
C–N stretching	1085.92 1043.49	1087.85	1074.35	1072.42	1070.49	1070.49
C–H asymmetric stretching	873.75	873.75	873.75	873.75	873.75	873.75
N–H out of plane bending (N–H wagging and twisting aliphatic 2° amine)/C–S bond	713.66 611.43 607.58	713.66 611.43 607.58	713.66 611.43 607.58	713.66 611.43 607.58	713.66 611.43 607.58	713.66 611.43 607.58
O–N=O bending/iron oxide	567.07	567.07	567.07	567.07	567.07	567.07
S–S stretching/iron oxide	536.21	536.21	536.21	536.21	536.21	536.21

MIN-SB, the decrease in intensity of the peaks was observed for N–H, C=O and COO<sup>−</sup> functional groups, whereas for MIN-amended sludge, the intensity of the peak increased. This indicates the involvement of these peaks in the retention of chromium ions and the possible metal binding on the adsorbents. The change in intensities was observed for the functional groups C–H, N–H, C–S, O–N=O and S–S, respectively. This indicates the involvement of these groups in the retention of chromium ions. Thus, in sludge amended by nanoparticles and nanobiocomposites, a change in intensities and shift of the peaks were observed, which can be attributed to intramolecular and intermolecular hydrogen bonding, steric effect and degree of conjugation occurring during chromium ion binding (Mohan et al. 2006).

### 3.5.2 XRD Study

The X-ray diffraction analysis of the unamended sludge and sludge amended by ZVIN, MIN, ZVIN-SB and MIN-SB was given in the supplementary file (Fig. S6). Table 5 shows the elements present in the unamended sludge and sludge amended by nanoparticles and nanobiocomposites. The presence of trivalent chromium in the sludge

is confirmed by higher intensity peaks observed in Figs. S6 (a) to S6 (f). The trivalent chromium ions found in the sludge are chromium nitrate hydrate (Cr(NO<sub>3</sub>)<sub>3</sub>·9H<sub>2</sub>O), chromium chloride (CrCl<sub>3</sub>), chromium oxide hydroxide (CrOOH), chromium hydroxide hydrate (Cr(OH)<sub>3</sub>·3H<sub>2</sub>O) and chromium sulfate (Cr<sub>2</sub>(SO<sub>4</sub>)<sub>3</sub>). The data show the presence of traceable amount of hexavalent chromium ions such as chromium carbonyl (C<sub>6</sub>CrO<sub>6</sub>) and ammonium chromium oxide ((NH<sub>4</sub>)<sub>2</sub>Cr<sub>2</sub>O<sub>7</sub>) in the unamended sludge and sludge amended by nanoparticles and nanobiocomposites. The other elements identified in the analysis are calcium oxalate hydrate (C<sub>2</sub>CaO<sub>4</sub>H<sub>2</sub>O, C<sub>4</sub>H<sub>4</sub>CaO<sub>6</sub>·4H<sub>2</sub>O), sodium chloride (NaCl), calcium carbonate (Ca(CO<sub>3</sub>)), calcium sulphate (Ca(SO<sub>4</sub>)), calcium hydroxide (Ca(OH)<sub>2</sub>). The addition of adsorbents has increased the intensity of iron hydroxide (FeOOH) and iron oxide (Fe<sub>2</sub>O<sub>3</sub>) in the sludge amended by nanoparticles and nanobiocomposites. Thus, the increased iron content in the sludge amended by nanoparticles and nanobiocomposites assisted the formation of more iron chromium oxide (FeCr<sub>2</sub>O<sub>4</sub>, Cr<sub>1.3</sub>Fe<sub>0.7</sub>O<sub>3</sub>) compounds. The formation of iron chromium oxide hydrate (Fe<sub>2</sub>Cr<sub>4</sub>O<sub>15</sub>·4H<sub>2</sub>O) in the

**Table 5** X-Ray diffraction analysis of unamended sludge and sludge amended by iron-based nanoparticles and nanobiocomposites

Elements	Raw sludge	Unamended sludge	ZVIN-amended sludge	MIN-amended sludge	ZVIN-SB-amended sludge	MIN-SB-amended sludge	JCPDS ID
	2θ values						
CrCl <sub>3</sub>	23.16	23.2, 66.31	23.16, 36.38	23.17	23.14	23.18	00-032-0279
Cr(NO <sub>3</sub> ) <sub>9</sub> ·9H <sub>2</sub> O	29.47, 31.74	29.53, 31.81	29.56, 31.83	29.48	29.49, 31.77	29.5, 31.76	00-031-0409
C <sub>2</sub> CaO <sub>4</sub> H <sub>2</sub> O	36.11, 45.59	31.52	30.02	36.13, 48.89	39.76	29.7	00-020-0231
C <sub>4</sub> H <sub>4</sub> CaO <sub>6</sub> ·4H <sub>2</sub> O	48.56	31.93	43.55	31.75	23.02	39.55	00-026-0330
C <sub>6</sub> CrO <sub>6</sub>	47.97	60.94	60.95	31.85	48.93	48.6	00-040-0751
(NH <sub>4</sub> ) <sub>2</sub> ·Cr <sub>2</sub> O <sub>7</sub>	47.72	36.16, 48.62	36.21	47.26	36.14	36.13	00-025-0029
NaCl	45.49	45.52, 56.53	45.56	45.46	45.5	45.48	00-005-0628
CaCO <sub>3</sub>	47.51, 57.5	47.66, 57.54, 64.91	48.64, 57.54	47.17	23.02	43.31, 64.86	00-005-0586
CaSO <sub>4</sub>	48.63	48.73	48.74	48.64	48.83	48.68	00-037-1496
Ca(OH) <sub>2</sub>	47.28	47.21	47.22	47.17	47.26	–	00-044-1481
Cr <sub>2</sub> (SO <sub>4</sub> ) <sub>3</sub>	39.55	57.73	47.67	47.26, 47.69	47.63, 47.55	47.65	00-031-0413
FeOOH	64.89	–	60.85	–	56.77	64.97	00-044-1415
Fe <sub>2</sub> O <sub>3</sub>	–	57.64	57.69	–	57.52, 57.61	43.45, 57.63	00-033-0664
Fe <sub>2</sub> O <sub>3</sub>	60.83	43.38	43.41	60.75	50.18	57.46	00-039-1346
FeCr <sub>2</sub> O <sub>4</sub>	43.3	75.32	75.32, 30.02	43.33	43.32	60.85	00-034-0140
Cr <sub>1.3</sub> Fe <sub>0.7</sub> O <sub>3</sub>	–	84.03	39.64, 84.08	39.55	64.76	39.6, 83.96	00-035-1112
CrOOH	–	–	–	–	–	75.27	00-020-0312
Cr(OH) <sub>3</sub> ·3H <sub>2</sub> O	60.91	56.53	26.75	56.59	60.87	–	00-016-0817
Fe <sub>2</sub> Cr <sub>4</sub> O <sub>15</sub> ·4H <sub>2</sub> O	–	–	23.25, 26.75	–	29.99	–	00-030-0648

ZVIN and ZVIN-SB amended sludge is due to the reaction between iron and chromium compounds.

### 3.5.3 EDX and SEM Analysis

The EDX and SEM analysis of raw sludge, unamended sludge and sludge amended by ZVIN, MIN, ZVIN-SB and MIN-SB was given in the supplementary file (Fig. S7). The EDX analysis shows the presence of oxygen, calcium, carbon, chromium, chloride, sodium, sulphur, aluminium, magnesium, silicon and iron in the raw sludge, unamended sludge/control and sludge amended by ZVIN, MIN, ZVIN-SB and MIN-SB (Figs. S7(a) to (f)). Apart from the above-specified elements, the EDX analysis showed some impurities in the samples. The elements oxygen, carbon and calcium contribute higher atomic percentage of weight in the unamended sludge and sludge amended by nanoparticles and nanobiocomposites when compared with other elements. The percentage contribution of these elements (oxygen, carbon and calcium) was found to be 92.76,

89.75, 90.75, 83.84, 88.11 and 86.88 %, respectively, for raw sludge, unamended sludge, ZVIN amended sludge, MIN amended sludge, ZVIN-SB amended sludge and MIN-SB amended sludge. The EDX analysis shows that the addition of iron-based nanoparticles and nanobiocomposites to the sludge have significantly increased the quantity of iron compound. This was evident from the atomic weight percentage of iron in the unamended sludge and sludge amended by nanoparticles and nanobiocomposites. The percentage contribution of iron in the unamended sludge was found to be 0.06 % whereas in the sludge amended by ZVIN, MIN, ZVIN-SB and MIN-SB, it was found to be 0.38, 0.52, 0.13 and 0.84 %, respectively. The inset of Figs. S7(a) to (f) shows the SEM image of the raw sludge, unamended sludge/control and sludge amended by ZVIN, MIN, ZVIN-SB and MIN-SB. The SEM analysis shows that nanoparticles and nanobiocomposites were mixed with the sludge reasonably well (inset in Figs. S7(c) to (f)). The image shows that the sludge amended by nanoparticles and nanobiocomposites was found to be more

agglomerated than the raw sludge (Fig. S7(a)) and the unamended sludge (Fig. S7(b)). This may be due to the binding of chromium ions on the surfaces of nanoparticles and nanobiocomposites.

### 3.5.4 CV Analysis

Figure 7a, b shows the cyclic voltammetry curves respectively for  $\text{Cr}^{3+}$  standard solution (250 mg/L) and sludge extractants (control or unamended sludge and sludge amended by nanoparticles and nanobiocomposites). The cyclic voltammetry curve proves the redox reaction of the unamended sludge and the sludge amended by nanoparticles and nanobiocomposites. The approximate anodic peak current of the control and the treated samples corresponds to the range of 1.33–1.38 V. The anodic peak current of trivalent chromium solution was also found to be in this range. This establishes the presence of chromium in trivalent state. Similar results were obtained by Chatterjee et al. (2011), when the cyclic voltammetry analysis

for the removal of toxic  $\text{Cr}^{6+}$  by *Pseudomonas aeruginosa* was studied. The study confirmed the reduction of  $\text{Cr}^{6+}$  to  $\text{Cr}^{3+}$  at 1.33 V. Salimi et al. (2015) observed that, as the trivalent chromium concentration increased, the anodic peak current increased from 0.7 V (40  $\mu\text{mol/L}$ ) to 0.85 V (360  $\mu\text{mol/L}$ ). Katz and Salem (1993) studied the standard potential for oxidation-reduction equilibria for different chromium valence states. They suggested that, when the potential was 1.38 V, the half-cell reaction validated the presence of trivalent chromium. The CV result obtained in this study agrees with the observations made in other studies mentioned above.

## 4 Conclusions

The maximum retention capacity of chromium by the adsorbents in the sludge was found to be 69.9, 72, 77 and 100 %, respectively, for ZVIN, MIN, ZVIN-SB and MIN-SB. The maximum retention response of the nanoparticles and nanobiocomposites was obtained when the pH, adsorbent dosage and time were respectively 7, 100 g/kg and 48 h. The mobility of chromium ions from the unamended sludge and sludge amended by nanoparticles and nanobiocomposites was analyzed through batch study with three different desorbing media such as 0.1 N HCL, DIW and 0.1 N NaOH. The 100 % retention of chromium ions were observed by the sludge amended by ZVIN, MIN, ZVIN-SB and MIN-SB in acidic and neutral condition. In basic condition, the 100 % retention of chromium ions was not achieved even after 216 h. At equilibrium time (168 h), the percentage of retention was found to be 97.84, 98, 98.21 and 98.78 %, respectively, for ZVIN, MIN, ZVIN-SB and MIN-SB. In column study, the percentage of retention by the adsorbents was found to be 80.49, 92.5, 88.4 and 95.74 %, respectively, for ZVIN, MIN, ZVIN-SB and MIN-SB of chromium in the cumulative leachate concentration.

Adsorption data of chromium by the adsorbents fitted well with pseudo-first-order kinetic model with calculated adsorption capacity of 427.686, 521.078, 577.004 and 596.232 mg/kg, respectively, for ZVIN, MIN, ZVIN-SB and MIN-SB. Zero-order kinetics accurately predicted the experimental desorption capacity ( $q_e$ ) of the sludge amended by ZVIN, MIN, ZVIN-SB and MIN-SB. The calculated desorption capacity  $q_{e,cal}$  was found to be the highest in basic environment and the

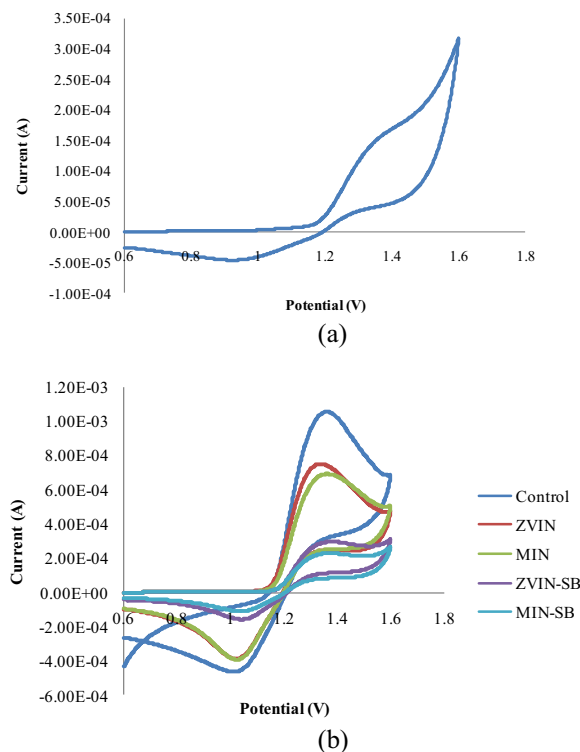


**Fig. 7** Cyclic voltammetry of **a** 250 mg/L of  $\text{Cr}^{3+}$  solution and **b** extractants from unamended sludge and sludge amended by nanoparticles and nanobiocomposites

least in acidic environment, and  $q_{e,cal}$  in the neutral condition was in between. Among all the adsorbents, MIN-SB has higher retention capacity and the desorption of chromium ions from MIN-SB amended sludge was found to be less than that from the sludge amended by ZVIN, MIN and ZVIN-SB. From FTIR study, the stretch and shift of the functional groups N–H, O–H, C=O, CH<sub>3</sub>, COO<sup>-</sup>, C–N, C–H, O–N=O, S–S in the sludge amended by ZVIN, MIN, ZVIN-SB and MIN-SB indicates the retention of chromium ions. Hence, nanoparticles and nanobiocomposites can be effectively used for immobilizing chromium in tannery sludge.

**Acknowledgments** The authors are thankful to the VIT University, Vellore, for providing sufficient facilities to carry out this research work. The first author is thankful to the Council of Scientific and Industrial Research (CSIR), New Delhi, India, for providing financial assistance to her as a Senior Research Fellowship (SRF).

## References

- Ahmad, M., Hashimoto, Y., Moon, D. H., Lee, S. S., & Ok, Y. S. (2012). Immobilization of lead in a Korean military shooting range soil using eggshell waste: an integrated mechanistic approach. *Journal of Hazardous Materials*, 209–210, 392–401.
- An, B., & Zhao, D. (2012). Immobilization of As (III) in soil and groundwater using a new class of polysaccharide stabilized Fe–Mn oxide nanoparticles. *Journal of Hazardous Materials*, 211–212, 332–341.
- APHA. (1998). *Standard Methods for Examination of Water and Wastewater* (20th ed.). Washington, DC: American Public Health Association.
- Apte, A. D., Tare, V., & Bose, P. (2005). Oxidation of Cr(III) in tannery sludge to Cr(VI): field observations and theoretical assessment. *Journal of Hazardous Materials*, 121(1–3), 215–222.
- Apte, A. D., Tare, V., & Bose, P. (2006). Extent of oxidation of Cr(III) to Cr(VI) under various conditions pertaining to natural environment. *Journal of Hazardous Materials*, 128(2–3), 164–174.
- Basha, S., & Murthy, Z. V. P. (2007). Kinetic and equilibrium models for biosorption of Cr(VI) on chemically modified seaweed *Cystoseira indica*. *Process Biochemistry*, 42(11), 1521–1529.
- Cao, J., & Zhang, W. X. (2006). Stabilization of chromium ore processing residue (COPR) with nanoscale iron particles. *Journal of Hazardous Materials*, 132(2–3), 213–219.
- Cassano, A., Drioli, E., Molinari, R., & Bertolutti, C. (1996). Quality improvement of recycled chromium in the tanning operation by membrane processes. *Desalination*, 108(1–3), 193–203.
- Ceribasi, I. H., & Yetis, U. (2001). Biosorption of Ni(II) and Pb(II) by *Phanerochaete chrysosporium* from binary metal system kinetics. *Water SA*, 27(1), 15–20.
- Chang, G. R., Liu, J. C., & Lee, D. J. (2001). Co-conditioning and dewatering of chemical sludge and waste activated sludge. *Water Research*, 35(3), 786–794.
- Chatterjee, S., Ghosh, I., & Mukherjee, K. K. (2011). Uptake and removal of toxic Cr(VI) by *Pseudomonas aeruginosa*: physico-chemical and biological evaluation. *Current Science*, 101(5), 645–652.
- Cossich, E. S., Tavares, C. R., & Ravagnani, T. M. (2002). Biosorption of chromium (III) by *Sargassum* sp. *Biomass. Electronic Journal of Biotechnology*, 5(2), 133–137.
- Costa, M. (2003). Potential hazards of hexavalent chromate in our drinking water. *Toxicology and Applied Pharmacology*, 188(1), 1–5.
- Costa, M., & Klein, C. B. (2006). Toxicity and carcinogenicity of chromium compounds in humans. *Critical Reviews in Toxicology*, 36(2), 155–163.
- Covington, A. D. (1998). John Arthur Wilson Memorial Lecture: new tannages for the new millennium. *Journal of the American Leather Chemists Association*, 93, 168–182.
- Dang, Y. P., Dalal, R. C., Edwards, D. G., & Tiller, K. G. (1994). Kinetics of zinc desorption from vertisols. *Soil Science Society of America Journal*, 58(5), 1392–1399.
- Errais, E., Duplay, J., Darragi, F., Rabet, I. M., Aubert, A., Huber, F., & Morvan, G. (2011). Efficient anionic dye adsorption on natural untreated clay: kinetic study and thermodynamic parameters. *Desalination*, 275(1–3), 74–81.
- Farinella, N. V., Matos, G. D., & Arruda, M. A. Z. (2007). Grape bagasse as a potential biosorbent of metals in effluent treatments. *Bioresource Technology*, 98(10), 1940–1946.
- Fonglim, S., Zheng, Y. M., Zou, S. W., & Chen, J. P. (2008). Characterization of copper adsorption onto an alginate encapsulated magnetic sorbent by a combined FTIR, XPS, and mathematical modeling study. *Environmental Science & Technology*, 42(7), 2551–2556.
- Fonseca, B., Maio, H., Quintelas, C., Teixeira, A., & Tavares, T. (2009). Retention of Cr (VI) and Pb(II) on a loamy sand soil: kinetics, equilibria and breakthrough. *Chemical Engineering Journal*, 152(1), 212–219.
- Foo, K. Y., & Hameed, B. H. (2011). Preparation of activated carbon from date stones by microwave induced chemical activation: application for methylene blue adsorption. *Chemical Engineering Journal*, 170(1), 338–341.
- Franco, D. V., Silva, L. M. D., & Jardim, W. F. (2009). Reduction of hexavalent chromium in soil and ground water using zero-valent iron under batch and semi-batch conditions. *Water Air and Soil Pollution*, 197(1–4), 49–60.
- Gerente, C., Lee, V. K. C., Cloirec, P. L., & McKay, G. (2007). Application of chitosan for the removal of metals from wastewaters by adsorption-mechanisms and models review. *Critical Reviews in Environmental Science and Technology*, 37(1), 41–127.
- Gong, Y., Liu, X., Huang, L., & Chen, W. (2010). Stabilization of chromium: an alternative to make safe leathers. *Journal of Hazardous Materials*, 179(1–3), 540–544.
- Gu, H., Rapole, S. B., Sharma, J., Huang, Y., Cao, D., Colorado, H. A., Luo, Z., Haldolaarachchige, N., Young, D. P., Walters, B., Wei, S., & Guo, Z. (2012). Magnetic polyaniline

- nanocomposites toward toxic hexavalent chromium removal. *RSC Advances*, 2(29), 11007–11018.
- Gu, H., Rapole, S. B., Huang, Y., Cao, D., Luo, Z., Wei, S., & Guo, Z. (2013). Synergistic interactions between multi-walled carbon nanotubes and toxic hexavalent chromium. *Journal of Material Chemistry A*, 1(6), 2011–2021.
- Ho, Y. S., & Mckay, G. (1999). Pseudo second order model for sorption processes. *Process Biochemistry*, 34(5), 451–465.
- Katz, S. A., & Salem, H. (1993). The toxicology of chromium with respect to its chemical speciation: a review. *Journal of Applied Toxicology*, 13(3), 217–224.
- Kim, C. J., Yoon, H. S., Chung, K. W., Lee, J. Y., Kim, S. D., Shin, S. M., Lee, S. J., Joe, A. R., Lee, S. I., Yoo, S. J., & Kim, S. H. (2014). Leaching kinetics of lanthanum in sulfuric acid from rare earth element (REE) slag. *Hydrometallurgy*, 146, 133–137.
- Kumar, P. A., Ray, M., & Chakraborty, S. (2009). Adsorption behaviour of trivalent chromium on amine-based polymer aniline formaldehyde condensate. *Chemical Engineering Journal*, 149(1–3), 340–347.
- Kushwaha, S., Sreedhar, B., & Sudhakar, P. P. (2012). Adsorption of  $Hg^{2+}$  onto *Borassus Flabellifer*: a redox mechanism. *Chemical Engineering Journal*, 193–194, 328–338.
- Labib, M., Dukhin, S. S., & Tabani, Y. (2010). Desorption kinetics during capillary flow. *Colloids and Surfaces A: Physicochemical and Engineering Aspects*, 354(1), 45–50.
- Levenspiel, O. (1972). *Chemical Reaction Engineering* (Second ed., p. 357). New York: Wiley.
- Lu, W., Shen, Y., Xie, A., & Zhang, W. (2010). Green synthesis and characterization of superparamagnetic  $Fe_3O_4$  nanoparticles. *Journal of Magnetism and Magnetic Materials*, 322(13), 1828–1833.
- Lu, M., Zhang, Y. M., Guan, X. H., Xu, X. H., & Gao, T. T. (2014). Thermodynamics and kinetics of adsorption for heavy metal ions from aqueous solutions onto surface amino-bacterial cellulose. *Transactions of Nonferrous Metals Society of China*, 24(6), 1912–1917.
- Manohar, D. M., Krishnan, A. K., & Anirudhan, T. S. (2002). Removal of mercury (II) from aqueous solutions and chlor-alkali industry wastewater using 2-mercaptobenzimidazole-clay. *Water Research*, 36(6), 1609–1619.
- Mishra, P. C., & Patel, R. K. (2009). Removal of lead and zinc ions from water by low cost adsorbents. *Journal of Hazardous Materials*, 168(1), 319–325.
- Mohan, J. (2004). *Organic spectroscopy principles and applications* (2nd ed., pp. 76–95). New Delhi: Narosa publishing house.
- Mohan, D., Singh, K. P., & Singh, V. K. (2006). Trivalent chromium removal from wastewater using low cost activated carbon derived from agricultural waste material and activated carbon fabric cloth. *Journal of Hazardous Materials*, 135(1–3), 280–295.
- Nakayama, E., Kuwamoto, T., Tsurubo, S., & Fujinaga, T. (1981). Chemical speciation of chromium in seawater. *Analytica Chimica Acta*, 130, 401–404.
- Nandi, B. K., Goswami, A., & Purkait, M. K. (2009). Removal of cationic dyes from aqueous solutions by kaolin: kinetic and equilibrium studies. *Applied Clay Science*, 42(3–4), 583–590.
- Nielsen, S. S., Petersen, L. R., Kjeldsen, P., & Jakobsen, R. (2011). Amendment of arsenic and chromium polluted soil from wood preservation by iron residues from water treatment. *Chemosphere*, 84(4), 383–389.
- Park, D., Ahn, C. K., Kim, Y. M., Yun, Y. S., & Park, J. M. (2008). Enhanced abiotic reduction of Cr(VI) in a soil slurry system by natural biomaterial addition. *Journal of Hazardous Materials*, 160(2–3), 422–427.
- Porter, S. K., Scheckel, K. G., Impellitteri, C. A., & Ryan, A. J. (2004). Toxic metals in the environment: thermodynamic considerations for possible immobilization strategies for Pb, Cd, As, and Hg. *Critical Reviews in Environmental Science and Technology*, 34(6), 495–604.
- Qiu, B., Gu, H., Yan, X., Guo, J., Wang, Y., Sun, D., Wang, Q., Khan, M., Zhang, X., Weeks, B. L., Young, D. P., Guo, Z., & Wei, S. (2014a). Cellulose derived magnetic mesoporous carbon nanocomposites with enhanced hexavalent chromium removal. *Journal of Material Chemistry A*, 2(41), 17451–17462.
- Qiu, B., Xu, C., Sun, D., Wei, H., Zhang, X., Guo, J., Wang, Q., Rutman, D., Guo, Z., & Wei, S. (2014b). Polyaniline coating on carbonfiber fabrics for improved hexavalent chromium removal. *RSC Advances*, 4(56), 29855–29865.
- Qiu, B., Xu, C., Sun, D., Yi, H., Guo, J., Zhang, X., Qu, H., Guerrero, M., Wang, X., Noel, N., Luo, Z., Guo, Z., & Wei, S. (2014c). Polyaniline coated ethyl cellulose with improved hexavalent chromium removal. *ACS Sustainable Chemistry and Engineering*, 2(8), 2070–2080.
- Qiu, B., Wang, Y., Sun, D., Wang, Q., Zhang, X., Weeks, B. L., O'Connor, R., Huang, X., Wei, S., & Guo, Z. (2015a). Cr(VI) removal by magnetic carbon nanocomposites derived from cellulose at different carbonization temperatures. *Journal of Material Chemistry A*, 3(18), 9817–9825.
- Qiu, B., Xu, C., Sun, D., Wang, Q., Gu, H., Zhang, X., Weeks, B. L., Hopper, J., Ho, T. C., Guo, Z., & Wei, S. (2015b). Polyaniline coating with various substrates for hexavalent chromium removal. *Applied Surface Science*, 334, 7–14.
- Rashti, M. R., Esfandbod, M., Adhami, E., & Srivastava, P. (2014). Cadmium desorption behaviour in selected subtropical soils: effects of soil properties. *Journal of Geochemical Exploration*, 144, 230–236.
- Reddy, D. H. K., & Lee, S. M. (2013). Synthesis and characterization of a chitosan ligand for the removal of copper from aqueous media. *Journal of Applied Polymer Science*, 130(6), 4542–4550.
- Rivera-Utrilla, J., & Sanchez-Polo, M. (2003). Adsorption of Cr(III) on ozonized activated carbon. Importance of Cpi-cation interactions. *Water Research*, 37(14), 3335–3340.
- Salimi, A., Pourbahram, B., Majd, S. M., & Hallaj, R. (2015). Manganese oxide nanoflakes/multi-walled carbon nanotubes/chitosan nanocomposite modified glassy carbon electrode as a novel electrochemical sensor for chromium (III) detection. *Electrochimica Acta*, 156, 207–215.
- Sing, C., & Yu, J. (1998). Copper adsorption and removal from water by living mycelium of white-rot fungus *Phanerochaete chrysosporium*. *Water Research*, 32(9), 2746–2752.
- Singh, R., Misra, V., & Singh, R. P. (2011). Synthesis, characterization and role of zero-valent iron nanoparticle in removal of hexavalent chromium from chromium-spiked soil. *Journal of Nanoparticle Research*, 13(9), 4063–4073.
- Singh, R., Misra, V., & Singh, R. P. (2012). Removal of Cr(VI) by nanoscale zero-valent iron (nZVI) from soil contaminated



- with tannery wastes. *Bulletin of Environmental Contamination and Toxicology*, 88(2), 210–214.
- Tseng, J. Y., Chang, C. Y., Chang, C. F., Chen, Y. H., Chang, C. C., Ji, D. R., Chiu, C. Y., & Chiang, P. C. (2009). Kinetics and equilibrium of desorption removal of copper from magnetic polymer adsorbent. *Journal of Hazardous Materials*, 171(1–3), 370–377.
- Tseng, R. L., Wu, P. H., Wu, F. C., & Juang, R. S. (2011). Half-life and half-capacity concentration approach for the adsorption of 2, 4-dichlorophenol and methyl blue from water on activated carbons. *Journal of Taiwan Institute of Chemical Engineers*, 42(2), 312–319.
- Tunay, O., Kabdasli, I., Orhon, D., & Ates, E. (1995). Characterization and pollution profile of leather tanning industry in turkey. *Water Science and Technology*, 32(12), 1–9.
- Volesky, B., & Holan, Z. R. (1995). Biosorption of heavy metals. *Biotechnology Progress*, 11, 235–250.
- Wang, G. H., & Grathwohl, P. (2009). Activation energies of phenanthrene desorption from carbonaceous materials: column studies. *Journal of Hydrology*, 369(3), 234–240.
- Weber, W. J., & Smith, E. H. (1987). Simulation and design models for adsorption processes. *Environmental Science & Technology*, 21(11), 1040–1050.
- Wei, S., Wang, Q., Zhu, J., Sun, L., Lin, H., & Guo, Z. (2011). Multifunctional composite core–shell nanoparticles. *Nanoscale*, 3(11), 4474–4502.
- Xu, C., Qiu, B., Gu, H., Yang, X., Wei, H., Huang, X., Wang, Y., Rutman, D., Cao, D., Bhana, S., Guo, Z., & Wei, S. (2014). Synergistic interactions between activated carbon fabrics and toxic hexavalent chromium. *ECS Journal of Solid State Science and Technology*, 3(3), M1–M9.
- Zhang, D., Wei, S., Kaila, C., Su, X., Wu, J., Karki, A. B., Young, D. P., & Guo, Z. (2010). Carbon-stabilized iron nanoparticles for environmental remediation. *Nanoscale*, 2(6), 917–919.
- Zhu, J., Gu, H., Rapole, S. B., Luo, Z., Pallavkar, S., Haldolaarachchige, N., Benson, T. J., Ho, T. C., Hopper, J., Young, D. P., Wei, S., & Guo, Z. (2012a). Looped carbon capturing and environmental remediation: case study of magnetic polypropylene nanocomposites. *RSC Advances*, 2(11), 4844–4856.
- Zhu, J., Sadu, R., Wei, S., Chen, D. H., Haldolaarachchige, N., Luo, Z., Gomes, J. A., Young, D. P., & Guo, Z. (2012b). Magnetic graphene nanoplatelet composites toward arsenic removal. *ECS Journal of Solid State Science and Technology*, 1(1), M1–M5.
- Zhu, J., Wei, S., Gu, H., Rapole, S. B., Wang, Q., Luo, Z., Haldolaarachchige, N., Young, D. P., & Guo, Z. (2012c). One-pot synthesis of magnetic graphene nanocomposites decorated with core@double-shell nanoparticles for fast chromium removal. *Environmental Science and Technology*, 46(2), 977–985.
- Zhu, J., Wei, S., Chen, M., Gu, H., Rapole, S. B., Pallavkar, S., Ho, T. C., Hopper, J., & Guo, Z. (2013). Magnetic nanocomposites for environmental remediation. *Advanced Powder Technology*, 24(2), 459–467.
- Zhu, J., Gu, H., Guo, J., Chen, M., Wei, H., Luo, Z., Colorado, H. A., Yerra, N., Ding, D., Ho, T. C., Haldolaarachchige, N., Hopper, J., Young, D. P., Guo, Z., & Wei, S. (2014). Mesoporous magnetic carbon nanocomposite fabrics for highly efficient Cr(VI) removal. *Journal of Material Chemistry A*, 2(7), 2256–2265.